Stability of trapped solutions of a nonlinear Schrödinger equation with a nonlocal nonlinear self-interaction potential

Saxena, Avadh Behari
Cooper, Fred
Khare, Avinash
Dawson, John F
Charalampidis, E. G.

To be published in: Journal of Physics A: Mathematical and Theoretical

DOI to publisher's version: 10.1088/1751-8121/ac265b

Stability of trapped solutions of a nonlinear Schrödinger equation with a nonlocal nonlinear self-interaction potential

Stability of trapped solutions of a nonlinear Schrödinger equation with a nonlocal nonlinear self-interaction potential

Efstathios G. Charalampidis[1], Fred Cooper[2,3], Avinash Khare[4], John F. Dawson[5], Avadh Saxena[3]

[1]Mathematics Department, California Polytechnic State University, San Luis Obispo, CA 93407-0403, United States of America

[2]The Santa Fe Institute, 1399 Hyde Park Road, Santa Fe, NM 87501, United States of America

[3]Theoretical Division and Center for Nonlinear Studies, Los Alamos National Laboratory, Los Alamos, NM 87545, United States of America

[4]Physics Department, Savitribai Phule Pune University, Pune 411007, India

[5]Department of Physics, University of New Hampshire, Durham, NH 03824, United States of America

E-mail: echarala@calpoly.edu

E-mail: cooper@santafe.edu

E-mail: avinashkhare45@gmail.com

E-mail: john.dawson@unh.edu

E-mail: avadh@lanl.gov

Abstract. This work focuses on the study of the stability of trapped soliton-like solutions of a (1+1)-dimensional nonlinear Schrödinger equation (NLSE) in a nonlocal, nonlinear, self-interaction potential of the form $[\,|\psi(x,t)|^2+|\psi(-x,t)|^2\,]^\kappa$ where κ is an arbitrary nonlinearity parameter. Although the system with $\kappa=1$ (i.e., fully integrable case) was first reported by Yang (Phys. Rev. E 98 (2018) 042202), in the present work, we extend this model to the one in which κ is arbitrary. This allows us to compare the stability properties of the now trapped solutions to previously found solutions of the more usual NLSE with $\kappa\neq 1$ which are *moving* soliton solutions. We show that there is a simple, one-component, nonlocal Lagrangian and corresponding action governing the dynamics of the system. Using a collective coordinate method derived from the action as well as assuming the validity of Derrick's theorem, we find that these trapped solutions are stable for $0<\kappa<2$ and unstable when $\kappa>2$. At the critical value of κ, i.e. $\kappa=2$, the solution can either collapse or blowup linearly in time when $q_0=0$, where q_0 is the center of the initial density $\rho(x,t=0)=\psi^\star\psi$ of the solution. For $q_0\neq 0$ the displaced solution collapses. When $\kappa>2$ initial small displacements from the origin also lead to collapse of the wave function. This phenomenon is not seen in the usual NLSE.

August 24, 2021 8:58pm PDT have

LA-UR-21-20590

Submitted to: *J. Phys. A: Math. Theor.*

Keywords: Nonlocal nonlinear Schrödinger equation, variational approximation, collective coordinates, action principle, existence and spectral stability analysis.

1. Introduction

The nonlinear Schrödinger equation (NLSE) arises in many areas of physics including Bose-Einstein condensation, plasmas, water waves and nonlinear optics [1], among many others. A good summary of the history of the NLSE and its appearance and uses in many arenas is found in the article of Ablowitz and Prinari [2]. The NLSE in one spatial dimension is given by

$$\mathrm{i}\partial_t\psi(x,t) + \partial_{xx}\psi(x,t) + g\,|\psi(x,t)|^2\psi(x,t) = 0\,. \tag{1.1}$$

This has been generalized in the past to include arbitrary nonlinearity parameter κ (i.e. $2 \to 2\kappa$) and spatial dimension d in order to study the self-focusing property of solitary waves as a function of these two parameters (see for example the work by Rose and Weinstein in [3]). It was soon realized by Cooper, Lucheroni and Shepard [4], that the numerical results of Rose and Weinstein on the criteria for solitary wave blowup could be understood using a simple Gaussian trial wave function in Dirac's variational approach for obtaining the NLSE. Namely, using the fact that the NLSE can be considered as the stationary point of the Dirac action in d-dimensions:

$$\Gamma[\psi,\psi^*] \;= \int \mathrm{d}t\, L[\psi,\psi^*], \tag{1.2a}$$

$$L[\psi,\psi^*] \;= \frac{\mathrm{i}}{2}\int \mathrm{d}^d x\,[\,\psi^*(\partial_t\psi) - (\partial_t\psi^*)\psi\,] - H[\psi,\psi^*]\,, \tag{1.2b}$$

$$H[\psi,\psi^*] = \int \mathrm{d}^d x\,[\,(\partial_x\psi^*)(\partial_x\psi) - g\,(\psi^*\psi)^{\kappa+1}/(\kappa+1)]\,, \tag{1.2c}$$

and inserting a time-dependent Gaussian trial wave function for $\psi(x,t)$, the equations derived for the variational parameters enabled one to determine quite accurately the critical mass of the solitary wave needed for blowup as a function of κd when compared to the numerics. In Eq. (1.2), the nonlinearity is generalized to arbitrary κ and the dimension to arbitrary d as in Ref. [4]. Later trial wave functions of a post-Gaussian type led to even better agreement with numerical simulations [5].

More recent applications of the variational approach have considered trial wave functions based on the exact solitary wave solutions of the NLSE in the absence of external forces to study situations where the solitary waves have been placed in external potentials both real and complex. For complex potentials, a dissipation functional approach has been used in [6]. In this approach, one utilizes trial wave functions which promote the parameters of the unperturbed solitary wave solutions to become time dependent, as well as introduces time dependent conjugate variables in the phase of the trial wave functions. These time dependent parameters, called collective

coordinates (CCs) hereafter, are related to the low-order moments of the wave function and satisfy the exact low-order moment equations. In Ref. [6], it was shown that the dissipation functional method of obtaining the equations for the CCs was equivalent to an alternative approach of Quintero et al. of obtaining equations for CCs called the generalized traveling wave method [7]. More recently in Refs. [6, 8], the stability of exact solutions of a single component NLSE in a class of external potentials having supersymmetry ($\mathcal{SUSY}$) and parity-time, i.e., $\mathcal{PT}$ symmetry was studied. These results were then extended to two-component NLSEs in $\mathcal{PT}$-symmetric and supersymmetric external potentials in Refs. [9, 10]. The system consisting of two coupled NLSEs is called a Manakov system, and is completely integrable. Generalizing the nonlinearity to arbitrary nonlinearity to study the stability as a function of the nonlinearity power κ, this system is described by:

$$\{\, \mathrm{i}\,\partial_t + \partial_x^2 + 2\,g\,[\,|\psi_1(x,t)|^2 + |\psi_2(x,t)|^2\,]^\kappa\,\}\,\psi_1(x,t) = 0\,, \tag{1.3a}$$

$$\{\, \mathrm{i}\,\partial_t + \partial_x^2 + 2\,g\,[\,|\psi_1(x,t)|^2 + |\psi_2(x,t)|^2\,]^\kappa\,\}\,\psi_2(x,t) = 0\,. \tag{1.3b}$$

Manakov first investigated this system (i.e., Eqs. (1.3) for $\kappa = 1$) as a model for the propagation of electric fields in a waveguide [11]. Subsequently, the system was derived as a key model for lightwave propagation in optical fibers [12]. The possibility of experimentally coupling two-component NLSEs in matrix complex potentials has recently been investigated in nonlinear optics situations in which two waveguides are locally coupled through an antisymmetric medium [13].

The nonlocal, nonlinear Schrödinger equations (NNLSEs) that are currently being discussed in the literature are of two types. The original proposal of Ablowitz and Musslimani [14] replaced $\psi^*(x,t)$ in the NLSE for $\psi(x,t)$ with $\psi^*(-x,t)$ which now possesses $\mathcal{PT}$ symmetry. Here instead we follow Yang's suggestion [15] and set $\psi_2(x,t) = \psi_1(-x,t)$ in Eqs. (1.3). The NNLSE, its variants and soliton solutions, have been studied in a variety of physical contexts [14–30]. Specifically, the NNLSE finds applications in the context of self-induced potentials in classical optics, coupled waveguides and photonic lattices. Yang's proposal renders the system of Eqs. (1.3) *nonlocal*.

In this paper, we generalize these considerations by introducing an arbitrary nonlinearity with exponent denoted as κ hereafter (again, note that the resulting system is integrable only for $\kappa = 1$). In particular, we extend our previous discussion of two coupled NLSEs to the present case in order to compare the nonlocal stability results with those known for the usual one- and two-component *local* NLSEs. A major difference in the solution space is that when we impose the above mentioned constraint, there are no longer moving single solitary wave solutions; instead they are trapped at the origin. To study the effect of small distortions of the initial solution, we use a variational approximation as well as perform numerical simulations. Small perturbations on an exact solution cause a slight increase in the energy of the solution.

We find that the domains of stability with respect to blowup or collapse of the solutions in terms of the parameter κ are the same as those found for the solitons in

the usual Manakov system, whence instability occurs for $\kappa > 2$, and there is a critical "mass" for the width instability to occur when $\kappa = 2$. For $0 < \kappa < 2$ the behavior of the perturbed solutions is well captured by the small oscillation equations of the CC approach. Following our previous use of CCs, we introduce two pairs of canonically related collective coordinates: G and Λ which are related to the width parameter and its conjugate, and q and p related to the position and its conjugate variable. The CC approach also gives qualitative agreement for the motion of the perturbed soliton for all $\kappa > 0$ with what is found in numerical simulations of the NNLSE. The exact single solitary wave solution obeys the symmetry $\psi(x,t) = \psi(-x,t)$. However, once we perturb the solution away from the origin we break this symmetry and the behavior of the perturbed solution has to be determined by the full NNLSE. In the CC approach the parameters q and p break the parity symmetry, and allow us to study the effect of an initial small translation of the wave function. In the CC approach, we find that these parameters are stable for all values of $\kappa \in (0,2)$, in that $q(t)$ and $p(t)$ just make small oscillations around zero. This result is verified by numerical simulations of the NNLSE. For the critical value of $\kappa = 2$ as well as for $\kappa > 2$, having a small perturbation in q at $t = 0$ causes the solitary wave to collapse. In the regime $\kappa > 2$, choosing at $t = 0$, a small perturbation with $\dot{G} < 0$ (the dot stands for time differentiation) causes the wave function to blowup (i.e., the width goes to zero) at finite time; whereas choosing $\dot{G} > 0$ induces collapse of the wave function. The CCs for $q(t)$ and $p(t)$ behave quite differently in the NNLSE from those of the usual NLSE which has Galilean invariance.

The structure of the paper is as follows. In Sec. 2 we present our generalized model and give the exact yet trapped solitary wave solutions to the coupled equations discussed therein. In Sec. 3, we discuss the derivation of the equations of motion from an action principle. The conservation laws resulting from the action are presented in Sec. 4. In Sec. 5 we use Derrick's theorem to show that for $\kappa > 2$ the solutions are unstable. We also study the stability of the solitary wave to translational perturbations using an energy argument and find that the solitary waves stay trapped. In Sec. 6, we consider a four collective coordinates (4CC) variational approximation and derive the associated equations of motion. We consider initial values where both $\dot{G}$ as well as the center of the wave are displaced from the exact solution. We compare the variational results with numerical simulations of the NNLSE. We find no evidence for a translational instability using either the 4CC equations or the (full) NNLSE equation. Indeed, we show that the small oscillation equations derived from the CC equations describe the behavior of perturbations when $0 < \kappa < 2$, showing the stability of the exact solution, and that when $\kappa > 2$ the wave function either blows up or collapses. The new phenomenon found for this NNLSE, is that when we just perturb the position of the solitary wave for $\kappa \geq 2$, it leads to collapse of the wave function. We find that for blowup, there is a critical time which we can estimate, and for collapse, G grows linearly in time with a rate controlled by E/M where E and M are the conserved energy and mass of the wave, respectively.

In Sec. 7, we focus on the critical value of κ. Upon choosing a positive or negative value for the time derivative of the width parameter G leads to linear collapse or blowup.

The effect of a small initial displacement $q_0 := q(t=0)$ of the center of wave function leads to collapse of the wave function. In Sec. 8 we explain our numerical approach and then compare the numerical results to those of the CC approximation. Finally we state our main conclusions in Sec. 9.

2. The nonlocal and nonlinear Schrödinger equation: Yang's version and exact solutions

In [15], special solutions ($\kappa = 1$) of the Manakov system given by Eq. (1.3) were studied. Upon imposing the solution constraint

$$\psi_2(x,t) = \psi_1(-x,t)\,, \tag{2.1}$$

the system of Eqs. (1.3) reduces to the single nonlinear and nonlocal Schrödinger equation (NNLSE) of the form:

$$\{\, i\,\partial_t + \partial_x^2 + 2\,g\,[\,|\psi(x,t)|^2 + |\psi(-x,t)|^2\,]^\kappa\}\,\psi(x,t) = 0\,, \tag{2.2}$$

where now $\psi(x,t) \equiv \psi_1(x,t)$. The solitary wave solution to Eq. (2.2) for arbitrary κ can be found explicitly, and is given by

$$\psi(x,t) = A(\beta,\gamma)\,\mathrm{sech}^\gamma(\beta x)\,\mathrm{e}^{\mathrm{i}\,\omega\,t}\,, \quad \gamma = 1/\kappa\,, \tag{2.3}$$

provided that

$$\omega = (\gamma\beta)^2\,, \quad 2g\,[\,2A^2(\beta,\gamma)\,]^{1/\gamma} = \beta^2\,\gamma(\gamma+1)\,, \tag{2.4}$$

or, explicitly

$$A(\beta,\gamma) = \frac{1}{\sqrt{2}}\left[\,\frac{\beta^2\,\gamma(\gamma+1)}{2g}\,\right]^{\gamma/2}, \tag{2.5}$$

with β being kept arbitrary. We also note in passing that the case with $\kappa = 1$ is integrable in terms of the Inverse Scattering Transform (IST). The NNLSE is a Hamiltonian dynamical system for all κ. It is integrable only for $\kappa = 1$. At arbitrary κ it only has a few conservation laws.

Indeed, upon using the IST, Yang in [15] found not only one-soliton solutions of the form:

$$\psi(x,t) = \frac{\beta}{\sqrt{2}}\,\mathrm{sech}(\beta x)\,\mathrm{e}^{\mathrm{i}\,\beta^2\,t} \tag{2.6}$$

but also two- and three-soliton solutions of the NNLSE, all for $g = 1$ (the focusing case) and $\kappa = 1$ (integrable case). For this choice of the parameters (i.e., $g = \kappa = 1$), Eq. (2.3) agrees with Eq. (2.6). It should also be noted that the constraint given by Eq. (2.1) is different from the one first suggested by Ablowitz and Musslimani in [14, 16]; they considered a different system consisting of two coupled NLSEs, namely:

$$\{\quad \mathrm{i}\,\partial_t + \partial_x^2 + 2\,g\,\psi_1(x,t)\,\psi_2(x,t)\,\}\,\psi_1(x,t) = 0\,, \tag{2.7a}$$

$$\{\,-\mathrm{i}\,\partial_t + \partial_x^2 + 2\,g\,\psi_2(x,t)\,\psi_1(x,t)\,\}\,\psi_2(x,t) = 0\,. \tag{2.7b}$$

Imposing the solution constraint: $\psi_2(x,t) = \psi_1^*(-x,t)$, Eqs. (2.7) reduce to the single nonlocal and nonlinear equation:

$$\{\, \mathrm{i}\,\partial_t + \partial_x^2 + 2\,g\,\psi(x,t)\,\psi^*(-x,t)\,\}\,\psi(x,t) = 0\,. \tag{2.8}$$

The advantage of the system proposed by Yang is that it is accessible in nonlinear optics, and the first three conserved quantities are real by construction. Also the stability of the solutions can be studied by using the same techniques as the ones we used for the usual two-component NLSEs [8].

3. Action principle

The Manakov system of Eq. (1.3) can be written in vector form as

$$\{\, \mathrm{i}\,\partial_t + \partial_x^2 + 2\,g\,[\,\Psi^\dagger(x,t)\,\Psi(x,t)\,]^\kappa\,\}\,\Psi(x,t) = 0\,, \tag{3.1}$$

with

$$\Psi(x,t) = \begin{pmatrix} \psi_1(x,t) \\ \psi_2(x,t) \end{pmatrix} \in \mathbb{C}^2\,. \tag{3.2}$$

It can be shown that Eq. (3.1) can be derived from an action principle. Indeed, let

$$\Gamma[\Psi^\dagger,\Psi] = \int \mathrm{d}t\, L[\Psi^\dagger,\Psi] \tag{3.3}$$

be the action of the system where L stands for its Lagrangian given by

$$L[\Psi^\dagger,\Psi] = T[\Psi^\dagger,\Psi] - H[\Psi^\dagger,\Psi]\,, \tag{3.4}$$

with

$$T[\,\Psi^\dagger,\Psi\,] = \int \mathrm{d}x\,\frac{\mathrm{i}}{2}\left\{\,\Psi^\dagger(x,t)[\,\partial_t\Psi(x,t)\,] - [\,\partial_t\Psi^\dagger(x,t)\,]\,\Psi(x,t)\,\right\}, \tag{3.5a}$$

$$H[\,\Psi^\dagger,\Psi\,] = \int \mathrm{d}x\left\{\,|\,\partial_x\Psi(x,t)\,|^2 - \frac{2\,g}{\kappa+1}\,[\,\Psi^\dagger(x,t)\Psi(x,t)\,]^{\kappa+1}\right\}. \tag{3.5b}$$

Once we impose the constraint of Yang, then Eq. (2.2) can be obtained from the following nonlocal yet one-component action principle:

$$S[\psi,\psi^*] = \int \mathrm{d}t\, L[\psi,\psi^*]\,, \quad \{\,\psi,\psi^*\,\} \in \mathbb{C}\,, \tag{3.6}$$

$$L[\psi,\psi^*] = T[\psi,\psi^*] - H[\psi,\psi^*]\,, \tag{3.7}$$

with

$$T[\,\psi,\psi^*\,] = \frac{\mathrm{i}}{2}\int \mathrm{d}x\left\{\,\psi^*(x,t)[\,\partial_t\psi(x,t)\,] - [\,\partial_t\psi^*(x,t)\,]\,\psi(x,t)\,\right\}, \tag{3.8a}$$

$$\begin{aligned} H[\,\psi,\psi^*\,] &= \int \mathrm{d}x\left\{\,|\,\partial_x\psi(x,t)\,|^2 - \frac{g}{\kappa+1}\,[\,|\psi(x,t)|^2 + |\psi(-x,t)|^2\,]^{\kappa+1}\right\}, \\ &= H_1 - H_2. \end{aligned} \tag{3.8b}$$

Here (taking $g > 0$) H_1 and H_2 are positive. We will choose in our simulations $g = 1$. This way, the Lagrange's equation of motion

$$\frac{\delta L[\psi,\psi^*]}{\delta\psi^*(x,t)} - \frac{\mathrm{d}}{\mathrm{d}t}\left[\,\frac{L[\psi,\psi^*]}{\delta\psi_t^*(x,t)}\,\right] = 0 \tag{3.9}$$

reproduces Eq. (2.2). Note that in the derivation here we used

$$\frac{\delta\psi(-x,t)}{\delta\psi(x',t')} = \delta(x+x')\,\delta(t-t')\,, \tag{3.10}$$

which provides a factor of $2\,g$ multiplying the nonlocal term. The existence of this action formulation immediately leads to the fact that the Hamiltonian H given by Eq. (3.8b) is conserved.

4. Conservation laws

It is straightforward to see from Eq. (2.2) that the mass

$$M = \int \mathrm{d}x\,|\psi(x,t)|^2 \tag{4.1}$$

is conserved for any initial condition. For the exact solution of (2.3), M is explicitly given by

$$M(\beta,\gamma) = \frac{1}{2\beta}\left[\frac{\gamma(\gamma+1)\,\beta^2}{2g}\right]^{\gamma} c_1(\gamma)\,, \tag{4.2}$$

where $c_1(\gamma)$ is given in Eq. (A.1a). In addition, the energy (or the Hamiltonian) given by Eq. (3.8b) is also conserved, and for the solution of Eq. (2.3), $E(\beta,\gamma)$ is given by

$$E(\beta,\gamma) = -M(\beta,\gamma)\,\beta^2\,\frac{\gamma^2(2\gamma-1)}{2\gamma+1} = -\frac{\beta}{2}\,\frac{\gamma^2(2\gamma-1)}{2\gamma+1}\left[\frac{\gamma(\gamma+1)\,\beta^2}{2g}\right]^{\gamma} c_1(\gamma)\,. \tag{4.3}$$

It can be discerned from Eq. (4.3) that $E(\beta,\gamma) < 0$ for $\gamma > 1/2$ or $\kappa < 2$, and $E(\beta,\gamma) > 0$ for $\gamma < 1/2$ or $\kappa > 2$, and $E = 0$ for $\kappa = 2$. When $\kappa = 2$, the mass of the solution becomes independent of the width parameter β. In fact, we will show that when $\kappa = 2$, the exact solution has the critical mass, above which any initial wave function becomes unstable. At $g = 1$ and $\kappa = 2$, the mass reads

$$M = \frac{\pi}{4}\sqrt{\frac{3}{2}} = 0.9619123726213981\,, \tag{4.4}$$

which is independent of β, and (which we will find from our variational calculation) is equivalent to the critical mass. We note in passing that the parity operator has the effect: $\mathcal{P}\psi(x,t) = \psi(-x,t) = \pm\psi(x,t)$ which is satisfied by the exact solution of Eq. (2.3) to Eq. (2.2) (also note that the solution has even parity). Moreover, there are other conservation laws that are directly obtainable from the equations of motion for ψ_1 and ψ_2. These are the two pseudo-masses

$$\begin{aligned} M_{21} &= \int \mathrm{d}x\,\psi_2^*(x,t)\,\psi_1(x,t) = \int \mathrm{d}x\,\psi^*(-x,t)\,\psi(x,t)\,, \\ M_{12} &= \int \mathrm{d}x\,\psi_1^*(x,t)\,\psi_2(x,t) = \int \mathrm{d}x\,\psi^*(x,t)\,\psi(-x,t)\,. \end{aligned} \tag{4.5}$$

For the exact soliton solution [cf. Eq. (2.3)], these two pseudo-masses are equal, and also are equal to the regular mass. However, once we distort the initial state from the exact solution, these two conserved quantities are complex conjugates of one another.

5. Derrick's theorem

Derrick's theorem [31] states that a solitary wave solution of a *local* Hamiltonian dynamical system is *unstable* if it is unstable to scale transformations of the form: $x \mapsto \alpha x$ ($\alpha > 0$) when we keep the mass of the solitary wave fixed. Here, we are dealing with a nonlocal Hamiltonian. However the Lagrangian was derived from a *local* two-component Manakov system whose stability has been considered earlier by using Derrick's theorem [32]. Let us consider exact solitary wave solutions of the (separation of variables) form

$$\psi(x,t) = r(x)\,\mathrm{e}^{-\mathrm{i}\omega t}\,, \tag{5.1}$$

with an even $r(x)$, i.e., $r(-x) = r(x)$. If we let $x \to \alpha x$, then

$$\psi_\alpha(x,t) = \alpha^{1/2}\, r(\alpha x)\,\mathrm{e}^{-\mathrm{i}\omega t}\,, \tag{5.2}$$

which itself preserves the mass M given by

$$M = \int dx |\psi_\alpha(x,t)|^2 = \int dx |\psi(x,t)|^2. \tag{5.3}$$

Defining $H(\alpha)$ the value of H for the stretched solution, we have that

$$H(\alpha) \;= H_1(\alpha) - H_2(\alpha)\,, \tag{5.4a}$$

$$H_1(\alpha) = \int \mathrm{d}x\, |\partial_x \psi_\alpha(x,t)|^2 = \alpha^2 \int \mathrm{d}z\, |\partial_z r(z)|^2 > 0\,, \tag{5.4b}$$

$$\begin{aligned} H_2(\alpha) &= \frac{g}{\kappa+1} \int \mathrm{d}x\, [\, |\psi_\alpha(x,t)|^2 + |\psi_\alpha(-x,t)|^2\,]^{\kappa+1} \\ &= \frac{g\, 2^{\kappa+1}\alpha^\kappa}{\kappa+1} \int \mathrm{d}z\, [\, r^*(z)\, r(z)\,]^{\kappa+1} > 0\,, \end{aligned} \tag{5.4c}$$

and thus we can write it as

$$H(\alpha) = \alpha^2\, H_1 - \alpha^\kappa\, H_2\,, \qquad H_1 > 0\,, \qquad H_2 > 0\,. \tag{5.5}$$

The minimum of $H(\alpha)$ at $\alpha = 1$ is consistent with the equations of motion. From $\frac{\partial H(\alpha)}{\partial \alpha}\Big|_{\alpha=1} = 0$ one obtains $H_1 = (\kappa/2)\, H_2$. For stability, the second derivative of $H(\alpha)$ with respect to α and evaluated at $\alpha = 1$ must be positive:

$$\frac{\partial^2 H(\alpha)}{\partial \alpha^2}\bigg|_{\alpha=1} = 2\,(2-\kappa)\, H_1 \geq 0\,. \tag{5.6}$$

This result indicates that solutions are unstable to changes in the width, compatible with the conserved mass, when $\kappa > 2$. The case $\kappa = 2$ is a marginal case where it is known that blowup occurs at a critical mass [5].

The exact solution of the NNLSE, Eq. (2.3) indeed has the property that it extremizes $H(\alpha)$ at $\alpha = 1$. We find

$$H_1 = \frac{\gamma^2}{2\gamma+1}\,\frac{\beta}{2}\left[\,\frac{\gamma(\gamma+1)\beta^2}{2\,g}\,\right]^\gamma c_1(\gamma)\,, \tag{5.7a}$$

$$H_2 = \frac{2\gamma^3}{2\gamma+1}\,\frac{\beta}{2}\left[\,\frac{\gamma(\gamma+1)\beta^2}{2\,g}\,\right]^\gamma c_1(\gamma)\,, \tag{5.7b}$$

which satisfies $H_1 = (\kappa/2)\, H_2$.

5.1. Translational Landscape

Using Derrick's theorem we explored whether the solution was a maximum or minimum of the energy landscape as a function of the stretching parameter α. Here, we would like to do a similar analysis to study whether the energy increases or decreases as we let $x \to x+a$ where a is a small translation. Again we will posit that there is a translational instability if the energy $H[a]$ decreases as a departs from zero. Let us again consider the NNLSE defined in Eqs. (1.3a)-(1.3b). We want to see how the energy of the system changes under the translation $x \to x+a$ with the normalization fixed by the requirement that the mass is unchanged. This criterion was used to study the stability of solutions of the NLSE trapped in a Pöschl-Teller potential [33]. Clearly, $\psi \to \psi(x+a)$ preserves the mass of the wave function although it breaks the parity symmetry. The translated solution is given by:

$$\psi(x+a,t) = A(\beta,\gamma)\,\mathrm{sech}^{\gamma}[\beta(x+a)]e^{i\omega t}\,, \quad \gamma = 1/\kappa\,. \tag{5.8}$$

It is also clear that H_1 remains unchanged under $x \to x+a$. Only H_2 is not translationally invariant since

$$H_2 = -\frac{g}{\kappa+1}\int_{-\infty}^{\infty} \mathrm{d}x\,[\,\mathrm{sech}^2(\beta(x-a)) + \mathrm{sech}^2(\beta(a+x))\,]^{\kappa+1}\,. \tag{5.9}$$

At small a, and setting $g=\beta=1$ for simplicity, we find (up to quadratic terms) that

$$H_2[a,\kappa] = a^2 2^{2\kappa+6}\kappa^2\,[\,{}_2F_1(1,-\kappa-2;\kappa+2;-1)-1\,]^2 - \frac{\sqrt{\pi}\,a 2^{\kappa+1}\,\Gamma(\kappa+1)}{(\kappa+1)\Gamma(\kappa+3/2)}\,, \tag{5.10}$$

where ${}_2F_1$ is a hypergeometric function. This potential is confining at all $\kappa > 0$. Thus on account of the trapping nature of the self-interaction, we do not expect that there is a translational instability. We indeed find that perturbed solutions just oscillate about the origin. However, because the translations couple to the width parameter, the displacement of the center of the initial wave function by q_0 will cause the solitary wave to collapse for $\kappa \geq 2$. Also, if one chooses $\kappa = 2$ and blowup initial conditions with $\Lambda < 0$, such a displacement of the center of the initial wave function accelerates the blowup phenomenon.

6. Four collective coordinate variational ansätz

Unlike the NLSE which is translation invariant as well as Galilean invariant, for the NNLSE, if we displace the position of the trapped solution, we no longer have an exact solution, and our initial condition for the wave function no longer has parity symmetry. However, one can ask what happens to such an initial condition? Does it just oscillate around the origin or does it escape the effective trap for some critical value of κ? What we find both from our variational approach as well as from numerical simulations is that the displaced solitary wave just oscillates around the origin independent of the value of κ. However, in the unstable regime, displacing the solitary wave from the origin induces collapse of the wave function.

In this section, we study the behavior of the displaced solution by choosing a parity-breaking, four collective coordinate (4CC) ansätz for our variational wave function of the form:

$$\tilde{\psi}(x,Q(t)) = A(t)\,\mathrm{sech}^{\gamma}[\,(x-q(t))/G(t)\,]\,\mathrm{e}^{\mathrm{i}\phi(x)}\,, \tag{6.1a}$$

$$\phi(x,Q(t)) = -\theta(t) + p(t)\,(x-q(t)) + \Lambda(t)\,(x-q(t))^2\,, \tag{6.1b}$$

which allows us to choose displaced initial conditions where $q(0) \neq 0$. The variational parameters are related to moments of the density as well as the moments of the momentum distribution (see Appendix B for details). This ansätz is similar to the time dependent Hartree-Fock approximation of quantum field theory if we replace the $\mathrm{sech}^{\gamma}[\,(x-q(t))/G(t)\,]$ term by the Gaussian $\exp[-(x-q(t))^2/G(t)]$. This ansätz has been used in the past to discuss the stability of solitary waves in the NLSE in *external* trapping potentials [6, 8], as well as solitary waves in two-component NLSE systems in external complex confining potentials [9]. Note that for the NNLSE, this ansatz, on account of the variables $q(t)$ and $p(t)$ does *not* satisfy the conservation laws for the pseudo-masses M_{12} and M_{21} [cf. Eqs. (4.5)], whereas the numerical solutions of the NNLSE do satisfy these conservation laws. This approximation *does* satisfy the conservation of the usual mass of the NLSE, namely

$$M = \int \mathrm{d}x\ |\tilde{\psi}(x,Q(t))|^2 = G(t)\,A^2(t)\,c_1(\gamma)\,, \tag{6.2}$$

where $c_1(\gamma)$ is given in Eq. (A.1a). This way, $A(t)$ and $G(t)$ are not independent variables, and we can set $A^2(t) = M/[\,G(t)\,c_1(\gamma)\,]$. One obtains the effective Lagrangian for the CCs

$$Q(t) = \{\, q(t), p(t), G(t), \Lambda(t), \phi(t)\,\} \tag{6.3}$$

by substituting this ansätz into the Lagrangian from which we obtain the NNLSE equation, namely Eq. (3.7). The phase $\phi(t)$ does not enter in the dynamics, and so it can be ignored. Thus, we are left with four variational parameters or CCs:

$$Q(t) = \{\, q(t), p(t), G(t), \Lambda(t)\,\}\,. \tag{6.4}$$

The Lagrangian in this case is given by

$$L[Q,\dot{Q}] = T[Q,\dot{Q}] - H[Q]\,, \tag{6.5}$$

where

$$T[Q,\dot{Q}] = M\left\{\, p\,\dot{q} - G^2\,\dot{\Lambda}\,\frac{c_2(\gamma)}{c_1(\gamma)}\,\right\}, \tag{6.6}$$

$$H[Q] \quad = M\left\{\, p^2 + 4\,G^2\Lambda^2\,\frac{c_2(\gamma)}{c_1(\gamma)} + \frac{1}{G^2}\left[\,1 - 2\,\gamma\left(\frac{G_0}{G}\right)^{1/\gamma-2} f(q/G,\gamma)\,\right]\frac{\gamma^2}{2\gamma+1}\,\right\}, \tag{6.7}$$

together with

$$f(z,\gamma) = \frac{2\gamma+1}{2^{1/\gamma+2}\,\gamma\,c_1(\gamma)}\int \mathrm{d}y\,\Big[\ \mathrm{sech}^{2\gamma}(y-z) + \mathrm{sech}^{2\gamma}(y+z)\,\Big]^{1/\gamma+1}\,, \tag{6.8}$$

where $G_0 := G(t=0)$. Note that the energy is conserved, and is given by:

$$E/M = p^2 + 4\,G^2\Lambda^2\,\frac{c_2(\gamma)}{c_1(\gamma)} + \frac{1}{G^2}\left[1 - 2\,\gamma\left(\frac{G_0}{G}\right)^{1/\gamma-2} f(q/G,\gamma)\right]\frac{\gamma^2}{2\gamma+1}\ . \quad (6.9)$$

Thus, the equations of motion are given by:

$$\begin{aligned}
\dot{q} &= 2\,p\,,\\
\dot{p} &= \frac{2\,\gamma^3}{2\gamma+1}\,\frac{1}{G^3}\left(\frac{G_0}{G}\right)^{1/\gamma-2} f'(q/G,\gamma)\,,\\
\dot{G} &= 4\,G\,\Lambda\,,\\
\dot{\Lambda} &= -4\,\Lambda^2 + \frac{\gamma^2}{2\gamma+1}\,\frac{c_1(\gamma)}{c_2(\gamma)}\\
&\quad\times\left\{\frac{1}{G^4}\left[1 - \left(\frac{G_0}{G}\right)^{1/\gamma-2} f(q/G,\gamma)\right] - \frac{\gamma\,q}{G^5}\left(\frac{G_0}{G}\right)^{1/\gamma-2} f'(q/G,\gamma)\right\}\ . \quad (6.10)
\end{aligned}$$

6.1. Small Oscillation Regime ($\kappa < 2$)

Let us consider $0 < \kappa < 2$. Since E/M is conserved, this conservation law [cf. Eq. (6.9)] prevents collapse ($G \to \infty$) as well as blowup ($G \to 0$). Thus for small perturbations of the CC parameters Λ, q from zero, one is in a small oscillation region. In the small oscillation regime, choosing $G_0 = 1$ for convenience, we have that (ignoring terms quadratic in δq)

$$f(z,\gamma) = 1; \quad f'(z,\gamma) = -4\frac{\gamma+1}{2\gamma+3}z\,. \quad (6.11)$$

So in that regime, we get the equations:

$$\begin{aligned}
\delta\dot{q} &= 2\delta p\,,\\
\delta\dot{p} &= -8\gamma^3\frac{\gamma+1}{(2\gamma+1)(2\gamma+3)}\delta q\,,\\
\delta\dot{G} &= 4\,\delta\Lambda\,,\\
\delta\dot{\Lambda} &= -\frac{\gamma\,(2\gamma-1)}{(2\gamma+1)}\,\frac{c_1(\gamma)}{c_2(\gamma)}\,\delta G\,, \quad (6.12)
\end{aligned}$$

together with the ones corresponding to the small oscillations:

$$\begin{aligned}
&\delta\ddot{G} + 4\frac{\gamma\,(2\gamma-1)}{(2\gamma+1)}\frac{c_1(\gamma)}{c_2(\gamma)}\delta G = 0,\\
&\delta\ddot{q} + 16\gamma^3\frac{\gamma+1}{(2\gamma+1)(2\gamma+3)}\delta q = 0\,. \quad (6.13)
\end{aligned}$$

We see that in this regime, the oscillations of the position and width are not coupled. Coupling only occurs when the wave function is collapsing or blowing up so that δG is not small. As far as the general behavior of the perturbed wave function is concerned, when $0 < \kappa < 2$ the period of oscillation of q and p slowly increases over the entire domain. Moreover, the oscillation frequency of the width goes to zero as $\kappa \to 2$ indicative of the

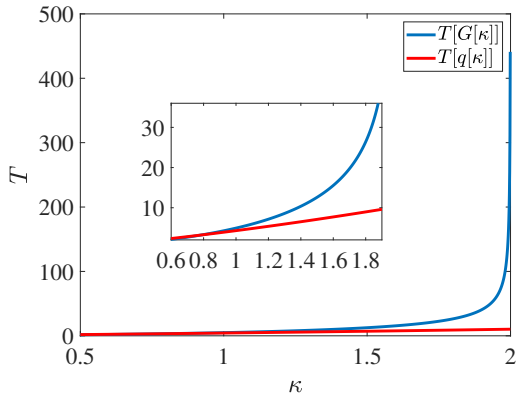

Figure 1. Period of G and q oscillations as a function of κ (the inset is a zoom-in) for the 4CC approximation.

instability setting in. This is seen in Fig. 1. Concerning the stability of this trapped solution, the small oscillation behavior at $\kappa = 1$, when the system becomes integrable, shows no special features.

As a typical example of how the solution in the stable regime responds to three different perturbations, we will look at the case $\kappa = 3/2$. The best agreement between the variational approximation and the numerical simulation occurs when we choose initial conditions that do not break parity; i.e. $p_0 = q_0$ (the subscript zero appearing in the CCs stands for their respective initial value, i.e., at $t = 0$). Then we find the results shown in Fig. 2.

To generate both small oscillations, we choose as initial conditions $q_0 = 1/100$ and $\Lambda_0 = -1/100$, and the respective results are shown in Fig. 3. Note that the period of oscillations is given by $T = \frac{2\pi}{\omega}$, and the period derived from the small oscillations equations give $T_q = 7.10774$ and $T_G = 12.5998$, respectively. Upon ignoring the effects of q from energy and mass conservation, one can determine the maximum value of G in the oscillatory regime as follows. At first, if we choose $p_0 = 0$ and $G_0 = 1$, the initial energy (divided by the conserved mass) is given by (ignoring tiny corrections to $f(0, \gamma) = 1$)

$$\frac{E}{M} = 4\,\Lambda_0^2\,\frac{c_2(\gamma)}{c_1(\gamma)} + \frac{1}{G^2}\left[1 - 2\,\gamma\right]\frac{\gamma^2}{2\gamma + 1}\,. \tag{6.14}$$

Note that the initial energy density depends only on Λ_0^2, so the oscillation frequencies are independent of the sign of Λ_0. The maximum value of G, denoted by G_m is reached when $\Lambda = 0$. So we have that G_m satisfies the equation

$$E(G_m, \gamma) = \left\{\frac{1}{G_m^2}\left[1 - 2\,\gamma\left(\frac{1}{G_m}\right)^{1/\gamma - 2}\right]\frac{\gamma^2}{2\gamma + 1}\right\}. \tag{6.15}$$

The maximum value of G for $\kappa = 3/2$ when we choose $\Lambda_0 = \pm 0.01, G_0 = 1$ is given

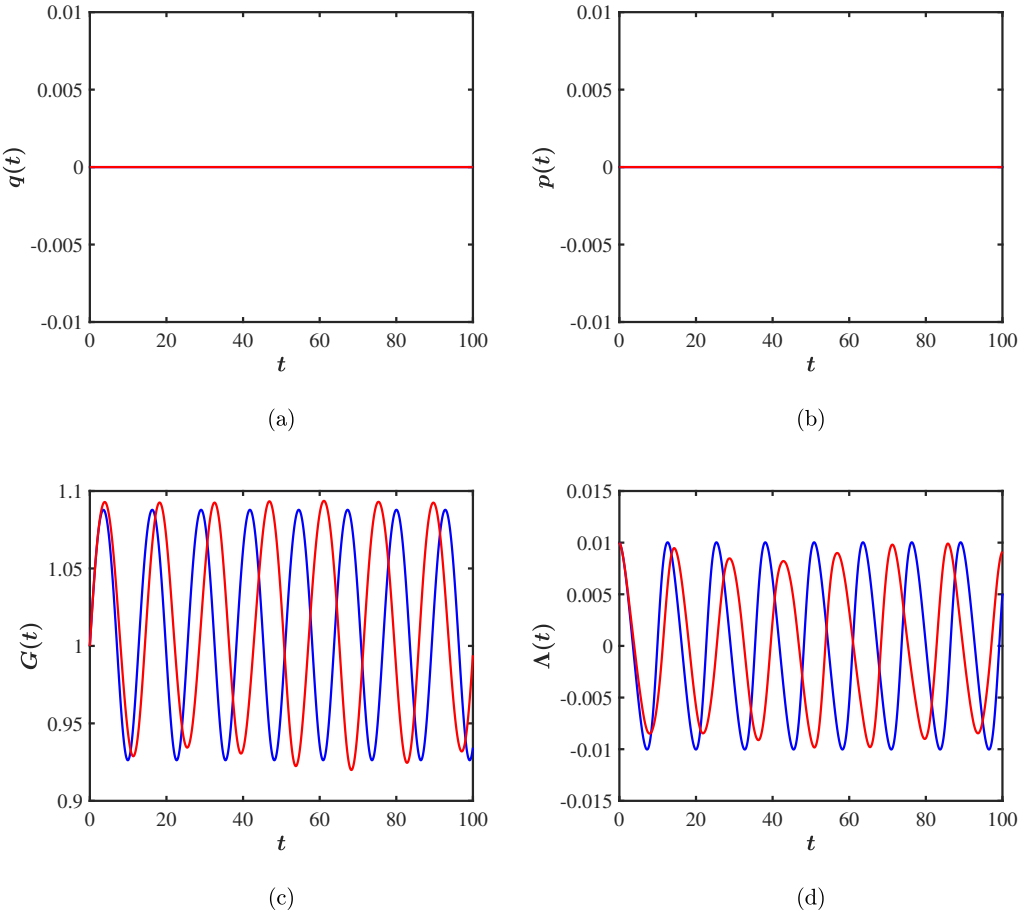

Figure 2. Dynamics for $\kappa = 1.5$ with $q_0 = 0$, $p_0 = 0$, $G_0 = 1$, and $\Lambda_0 = 0.01$. The variational results are shown in blue and the numerical ones (with $L = 10$) in red.

by $G_m = 1.087874$. This value of G_m is seen in both the CC approximation and in the numerical simulations as seen in Figs. 2 and 3. The disparity between the 4CC approximation and numerics for the variables q and p is due to the fact that for this case the 4CC approximation violates the two conservation laws, namely M_{21} and M_{12} (see Eqs. (4.5)). The final case of interest is to just displace the solution from the origin. This also generates via the coupling oscillations in G and Λ as well. The agreement with the numerical simulations is qualitatively good. (See Fig. 4). This third case is of course not found in the usual NLSE situation which in turn is translation invariant.

For the numerical simulations, we solve the NNLSE with initial conditions of $\psi(x, 0) = \tilde{\psi}(x, 0)$, for comparison. The numerical solutions were obtained by using MATLAB's `ODE113` integrator which is a variable-step, variable-order (VSVO) Adams-

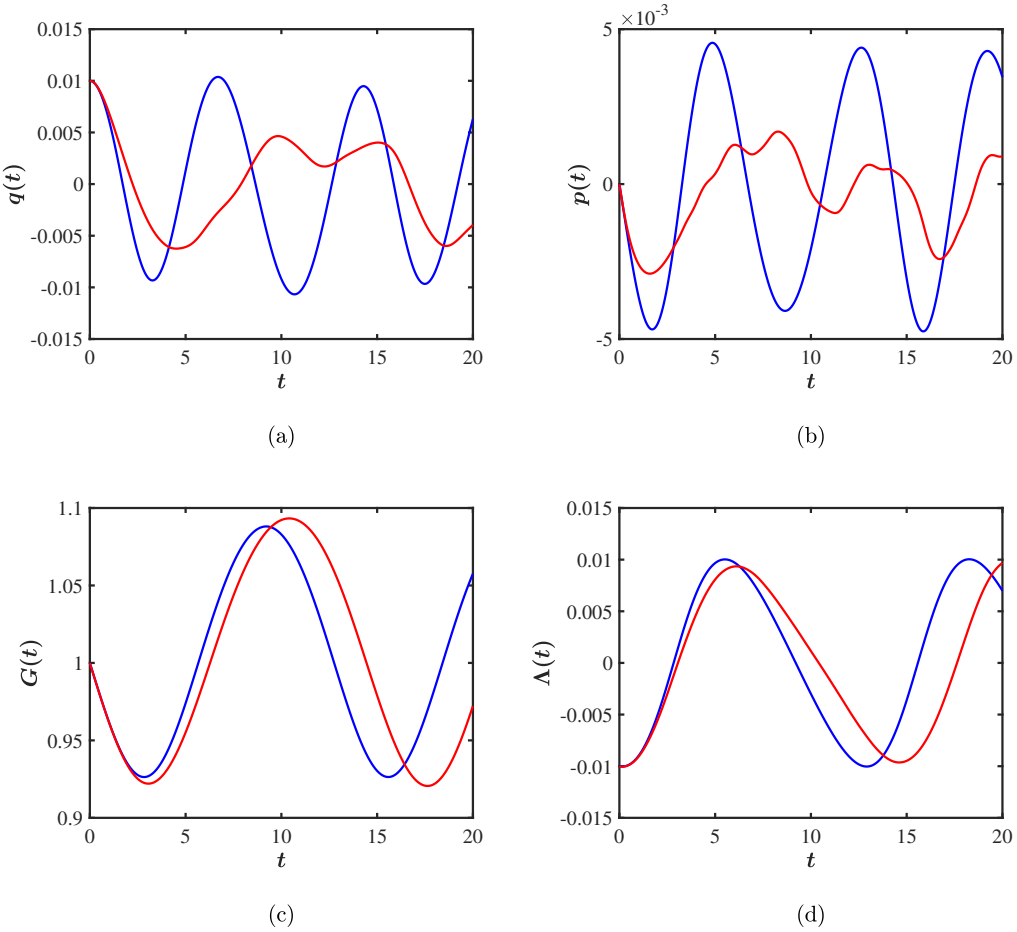

Figure 3. Dynamics for $\kappa = 1.5$ with $q_0 = 0.01$, $p_0 = 0$, $G_0 = 1$, and $\Lambda_0 = -0.01$. The variational results are shown in blue and the numerical ones (with $L = 10$) in red.

Bashforth method (see [34], and references therein). We solve the NNLSE on $x \in [-L, L]$ (where L is the domain's half-width) supplemented by zero Dirichlet boundary conditions (see the relevant figure captions for the values of L that were used). We should note in passing that the position of the boundary of the computational domain ($x = \pm L$) strongly depends on the initial condition. Indeed, the functional form of $\tilde{\psi}(x, 0)$ as $|x| \to L < \infty$ suggests tiny oscillations of the solution at the boundaries over time which are effectively considered to be of zero amplitude, i.e., zero Dirichlet boundary conditions. As per the spatial discretization, we considered a centered yet fourth-order accurate finite difference approximation. We further tested our numerical simulation results by considering other integrators and spatial discretizations such as the `ETDRK4` integrator and Fourier spectral collocation [35], and we obtained essentially

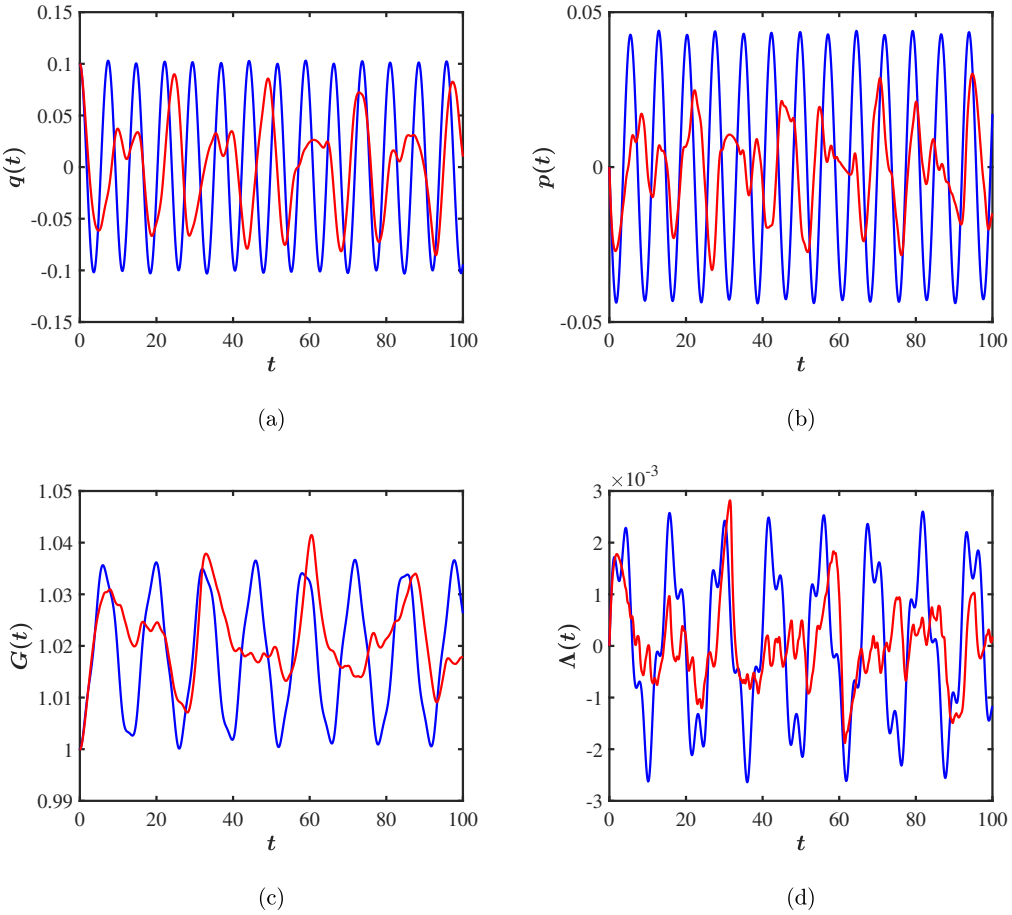

Figure 4. Dynamics for $\kappa = 1.5$ with $q_0 = 0.1$, $p_0 = 0$, $G_0 = 1$, and $\Lambda_0 = 0$. The variational results are shown in blue and the numerical ones (with $L = 10$) in red.

similar results.

6.2. Blowup or Collapse regime $\kappa > 2$

When $\kappa > 2$, choosing Λ ($\dot{G}$) positive or making a small displacement of the exact solution, $q_0 \neq 0$, leads to the collapse of the wave function. Choosing Λ positive leads to blowup of the perturbed trapped solution. First, let us look at the blowup regime from the CC perspective. Setting $q_0 = 0$ and also setting $G_0 = 1$, then from energy conservation and the equation of motion for $G(t)$, the scaled energy of Eq. (6.9) can be rewritten as:

$$\frac{E}{M} = \frac{\dot{G}^2}{4}\frac{c_2(\gamma)}{c_1(\gamma)} + \frac{1}{G^2}\,\frac{\gamma^2}{2\gamma+1} - \frac{2\,\gamma^3}{G^{1/\gamma}(2\gamma+1)}. \tag{6.16}$$

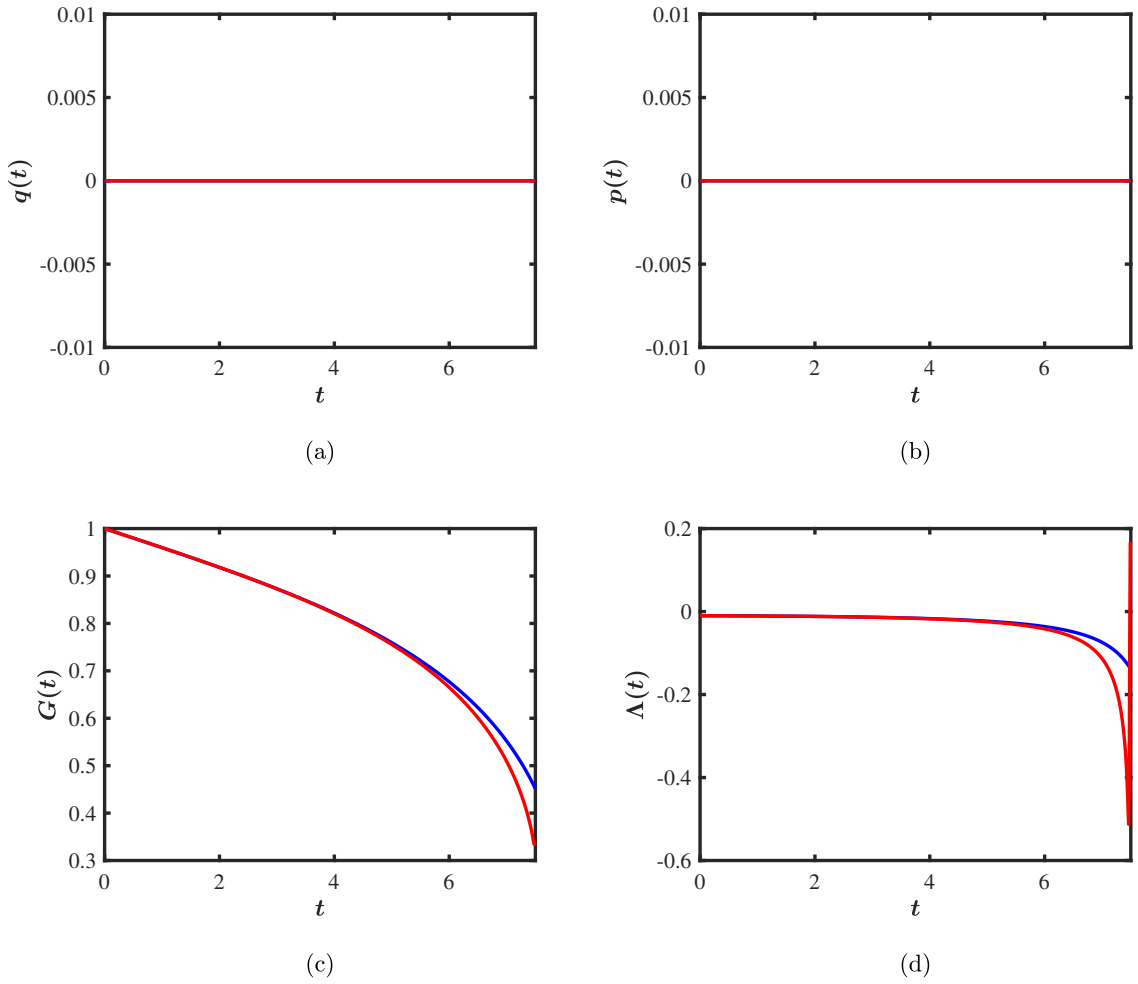

Figure 5. Dynamics when $\kappa = 2.2$ with $q_0 = 0$, $p_0 = 0$, $G_0 = 1$, and $\Lambda_0 = -0.01$. The numerical results in red (with $L = 30$) as well as the variational results in blue show blowup of the solution.

Upon rewriting the energy equation as

$$\dot{G}^2 = 4\,\frac{c_1(\gamma)}{c_2(\gamma)}\left(\frac{E}{M} + \frac{2\,\gamma^3}{G^{1/\gamma}(2\gamma+1)} - \frac{1}{G^2}\,\frac{\gamma^2}{2\gamma+1}\right), \tag{6.17}$$

and considering $G \to 0$, we can ignore the first and last terms, thus obtaining

$$\dot{G} = -\sqrt{\frac{c_1(\gamma)}{c_2(\gamma)}\frac{2\,\gamma^3}{G^{1/\gamma}(2\gamma+1)}} \tag{6.18}$$

for blowup. In other words, when we get near the critical time t^*, we have [5]

$$G(t) \propto (t - t^*)^{2/(\kappa+2)}\ . \tag{6.19}$$

This blowup behavior is seen both in the numerical simulations and variational approximation. For a typical case corresponding to $\kappa = 2.2$ and $\Lambda_0 = -1/100$, we obtain the result of Fig. 5.

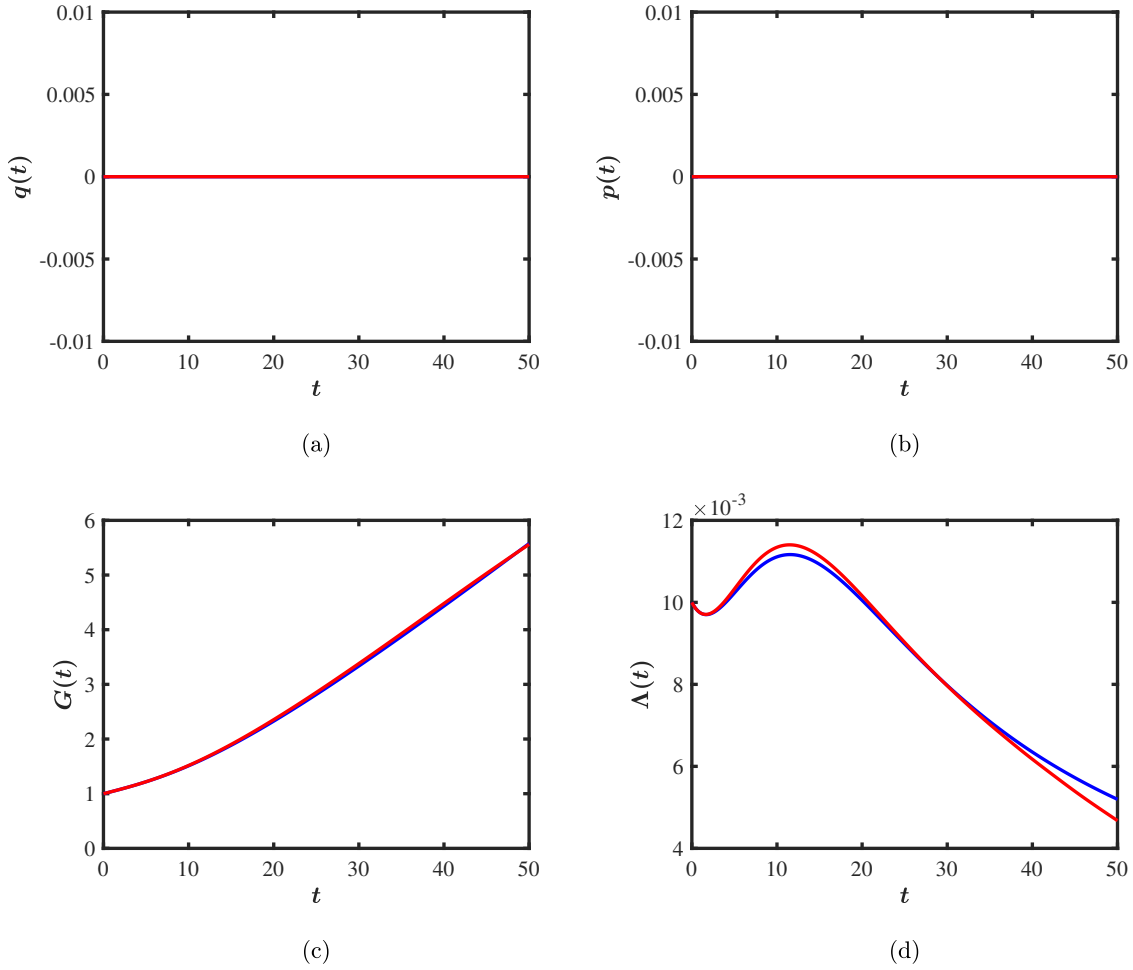

Figure 6. Dynamics when $\kappa = 2.2$ with $q_0 = 0$, $p_0 = 0$, $G_0 = 1$, and $\Lambda_0 = 0.01$. The numerical results in red (with $L = 30$) as well as the variational results in blue show a collapse.

If instead we choose $\Lambda_0 > 0$, then the solitary wave collapses. Once $G(t)$ gets large, only the first term in the energy equation becomes important. Therefore we find that asymptotically, the final value of $\dot{G}$ becomes a constant determined by the ratio E/M:

$$\frac{E}{M} = \frac{\dot{G}^2}{4}\frac{c_2(\gamma)}{c_1(\gamma)}\,. \tag{6.20}$$

This is borne out in the late time simulations of the collapse case. For $\kappa = 2.2$, and $\Lambda_0 = 1/100$ we obtain the result of Fig. 6. Finally we find a new phenomenon, not present in the NLSE equation in the unstable regime because there is no translation invariance, making a small translation of the initial state induces collapse of the wave function. This is not anticipated by Derrick's theorem. Because of the nonlinear coupling between q and G, one can initiate soliton collapse when $\kappa > 2$ by just giving q_0 a non-zero value. This is seen for two cases with $G_0 = 0.5$ in Fig. 7, and $G_0 = 1$ in Fig. 8.

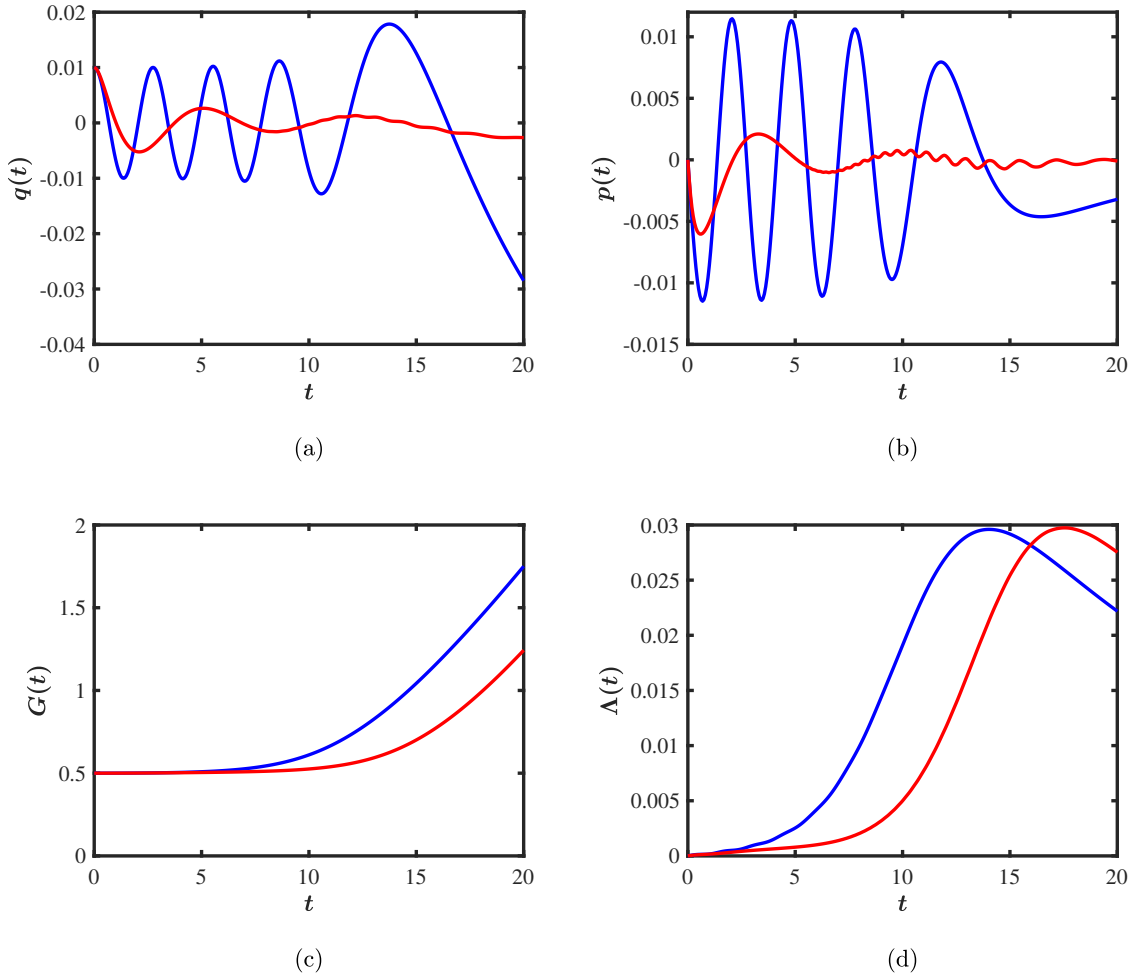

Figure 7. Dynamics when $\kappa = 2.1$ with $q_0 = 0.01$, $p_0 = 0$, $G_0 = 0.5$, and $\Lambda_0 = 0$. The variational results are shown in blue and the numerical ones (with $L = 30$) in red.

7. Behavior when $\kappa = 2$

When $\kappa = 2$, the exact solution is at the critical mass. So depending on how it is perturbed, it either collapses or blows up (linearly in time) if there are no perturbations in the position. When q_0 is not zero, and no perturbation is given to the width, then the wave function collapses. In the blowup case, since G can get large, having $q_0 \neq 0$ initially can alter the nature of the blowup. We will give examples below, with $\Lambda_0 = 0, \pm 0.01$ and $q_0 = 0.01$. The most interesting behavior is the collapse of the wave function when we give the initial wave function a slight translation. In that case, we get the result shown in Fig. 9. When $\Lambda > 0$, the wave function collapses linearly in time. When we add $q_0 \neq 0$, the collapse is slightly hastened, but now the periods of q and p *increase* in time when compared to the periodic regime. This is seen in Fig. 10. When $\Lambda < 0$, the wave function blows up ($G \to 0$) linearly in time. When we add $q_0 \neq 0$, the blowup is slightly hastened, but now the periods of q and p *decrease* in time when compared to the periodic regime. Both solutions fail at the blowup time. This is seen in Fig 11.

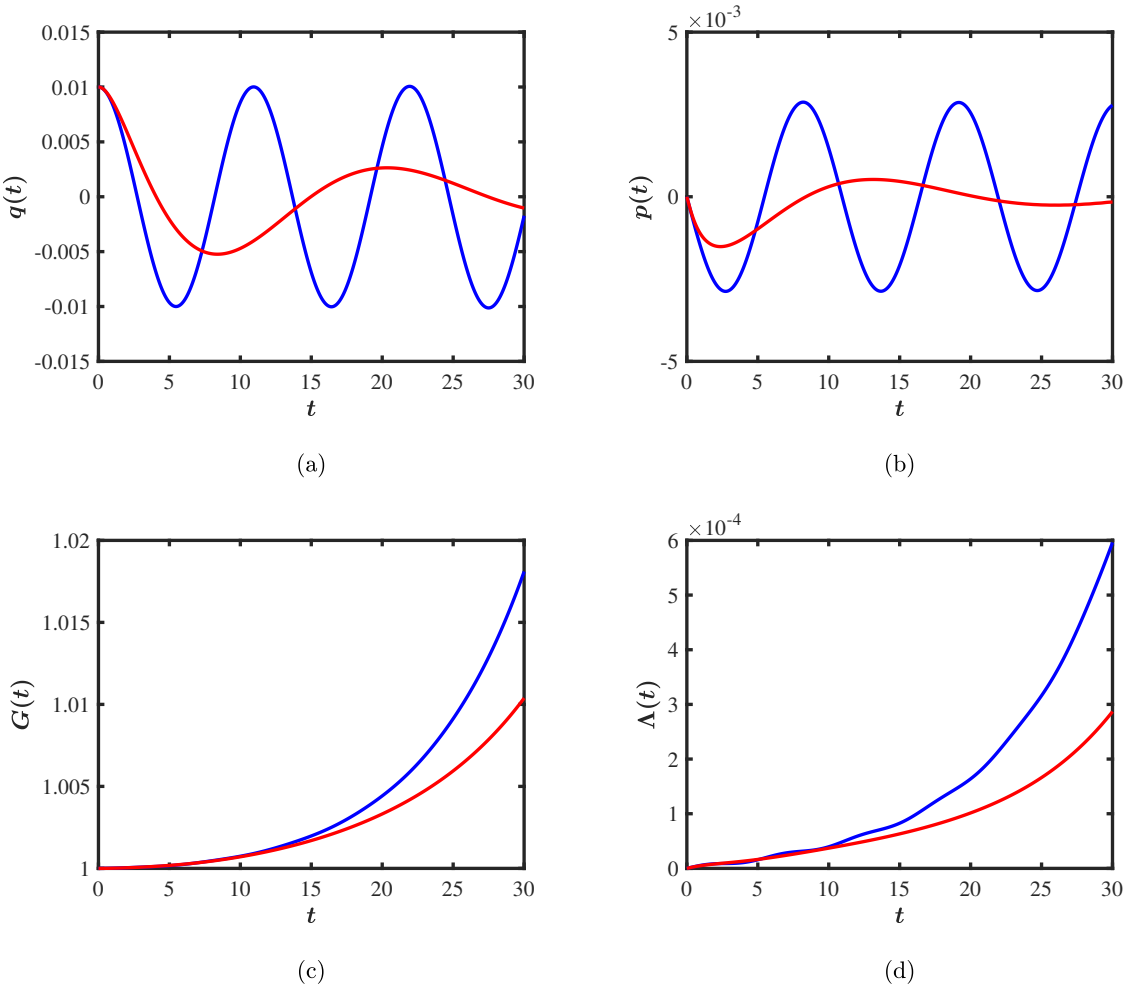

Figure 8. Dynamics when $\kappa = 2.1$ with $q_0 = 0.01$, $p_0 = 0$, $G_0 = 1$, and $\Lambda_0 = 0$. The variational results are shown in blue and the numerical ones in red (with $L = 80$).

8. Numerical simulations of the NNLSE

In this Section, we briefly discuss the stability and spatio-temporal evolution of the exact solution (2.3) to the NNLSE (2.2). To do so, we employ the separation of variables ansätz $\psi(x,t) = \psi^{(0)}(x)e^{\mathrm{i}\omega t}$, which is inserted into Eq. (2.2), thus obtaining:

$$\frac{\mathrm{d}^2\psi^{(0)}(x)}{\mathrm{d}x^2} + 2g\left[|\psi^{(0)}(x)|^2 + |\psi^{(0)}(-x)|^2\right]^{\kappa}\psi^{(0)}(x) - \omega\psi^{(0)}(x) = 0. \qquad (8.1)$$

Then, Eq. (8.1) is solved by means of a Newton-Krylov method as implemented in MATLAB with `nsoli` [36]. A sufficiently good initial guess to the nonlinear solver is provided by Eq. (2.3). Having identified a stationary solution $\psi^{(0)}(x)$ (upon convergence of `nsoli`), we perform a spectral stability analysis around it using the ansatz:

$$\widetilde{\psi}(x,t) = e^{\mathrm{i}\omega t}\left[\psi^{(0)}(x) + \varepsilon\left(a(x)e^{\lambda t} + b^*(x)e^{\lambda^* t}\right)\right], \quad \varepsilon \ll 1. \qquad (8.2)$$

Upon inserting Eq. (8.2) into Eq. (2.2), we arrive (at order $\mathcal{O}(\varepsilon)$) at the eigenvalue

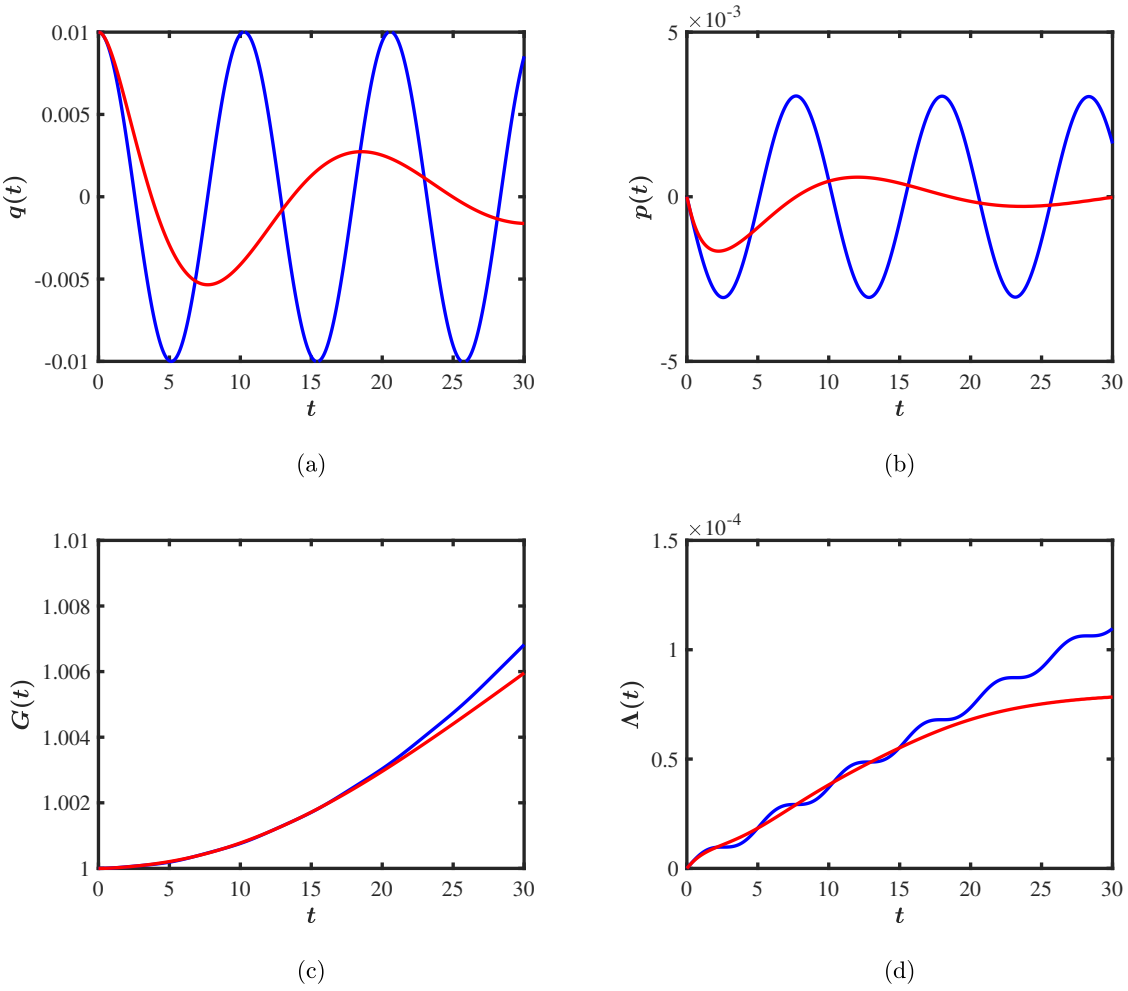

Figure 9. Dynamics when $\kappa = 2$ with $q_0 = 0.01$, $p_0 = 0$, $G_0 = 1$, and $\Lambda_0 = 0$. The numerical results in red (with $L = 80$) show collapse of the wave function in agreement with the variational results in blue.

problem of the form of

$$\begin{pmatrix} A_{11} & A_{12} \\ -A_{12}^* & -A_{11}^* \end{pmatrix} \begin{pmatrix} a \\ b \end{pmatrix} = \widetilde{\lambda} \begin{pmatrix} a \\ b \end{pmatrix}, \quad \widetilde{\lambda} = -\mathrm{i}\lambda, \tag{8.3}$$

with matrix elements given by

$$\begin{aligned} A_{11} = \frac{\mathrm{d}^d}{\mathrm{d}x^{\,2}} + 2g\Big\{ & \kappa \left[|\psi^{(0)}(x)|^2 + |\psi^{(0)}(-x)|^2\right]^{\kappa-1} \left[|\psi^{(0)}(x)|^2 + \psi_0(x)\psi_0^*(-x)\mathcal{P}\right] \\ & + \left[|\psi^{(0)}(x)|^2 + |\psi^{(0)}(-x)|^2\right]^{\kappa} \Big\} - \omega\,, \\ A_{12} = 2g\kappa & \left[|\psi^{(0)}(x)|^2 + |\psi^{(0)}(-x)|^2\right]^{\kappa-1} \left[\left(\psi^{(0)}(x)\right)^2 + \psi_0(x)\psi_0(-x)\mathcal{P}\right]\,, \end{aligned} \tag{8.4a}$$

where $\mathcal{P}$ stands for the space reflection operator, i.e., $\mathcal{P}f(x) = f(-x)$, for a general function $f(x)$.

The results of the eigenvalue problem [cf. Eq. (8.3)] are shown in Fig. 12 with $g = 1$ and $\beta = 1$. It can be discerned from the right panel of the figure, the emergence of a real

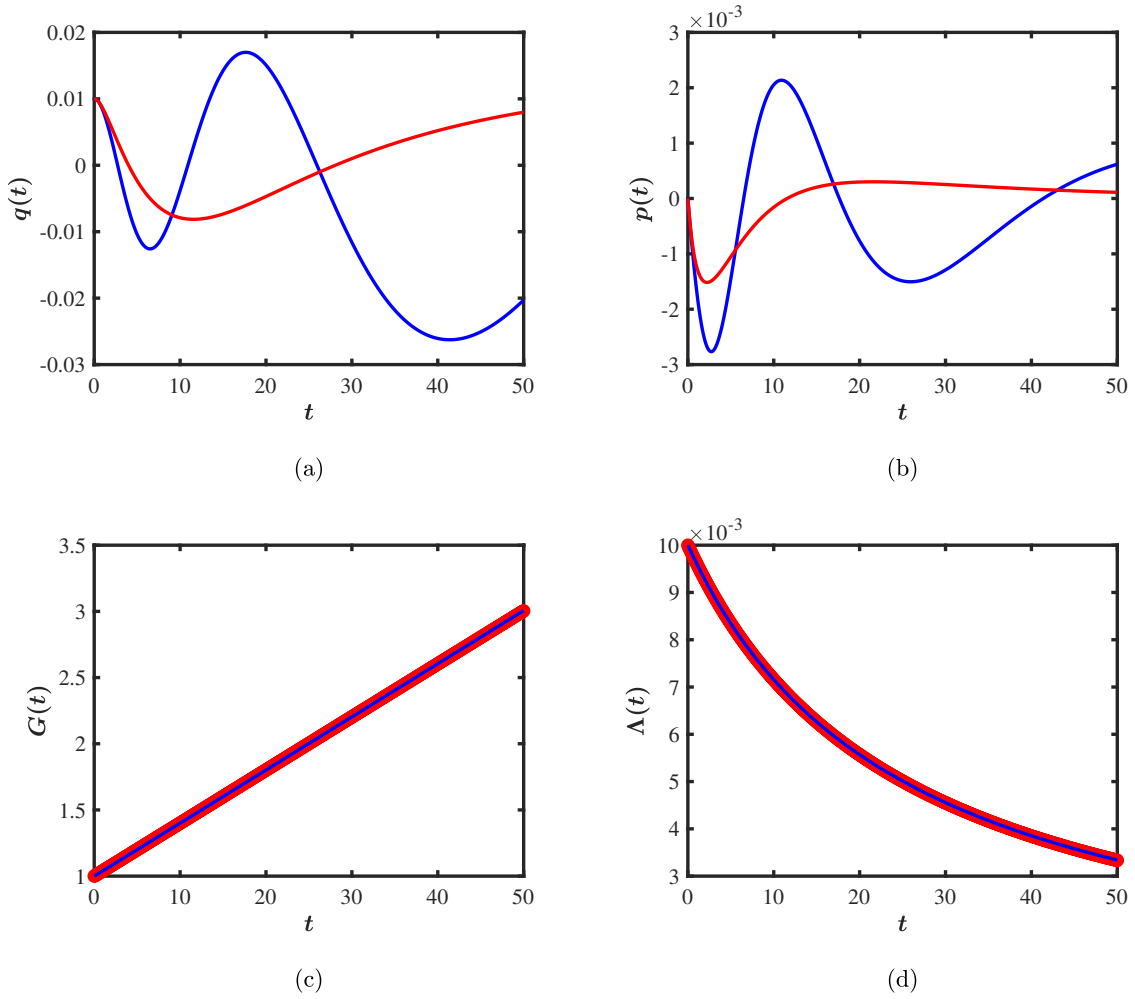

Figure 10. Dynamics when $\kappa = 2$ with $q_0 = 0.01$, $p_0 = 0$, $G_0 = 1$, and $\Lambda_0 = 0.01$. The numerical results (with $L = 80$) in red and the variational results in blue both describe collapse. Note that results from numerical simulations for the variables $G(t)$ and $\Lambda(t)$ are shown with red open circles to ease visualization.

eigenvalue at $\kappa = 2$, thus rendering the solution to be spectrally unstable (and similar to the local case). Although a detailed study and understanding of the underlying instability mechanism is of paramount importance (see, e.g., [37] as well as [38] and references therein), it is beyond the scope of the present work. Subsequently, Fig. 13 presents results on the spatio-temporal evolution of the exact solution for various values of κ. These numerical results were obtained by using a fourth-order accurate, central finite difference scheme for the (one-dimensional) Laplacian on a computational domain with half-width $L = 50$ and resolution $\Delta x = 0.1$. Note that Fig. 13(d) demonstrates an unstable solution (i.e., a blowup case), and the time integration was stopped when the full-width-at-half-maximum (FWHM) was less than Δx (for instance, the blow-up time happens at a later time $t_{\text{blowup}} \approx 474$ in this panel, as per the discretization employed herein).

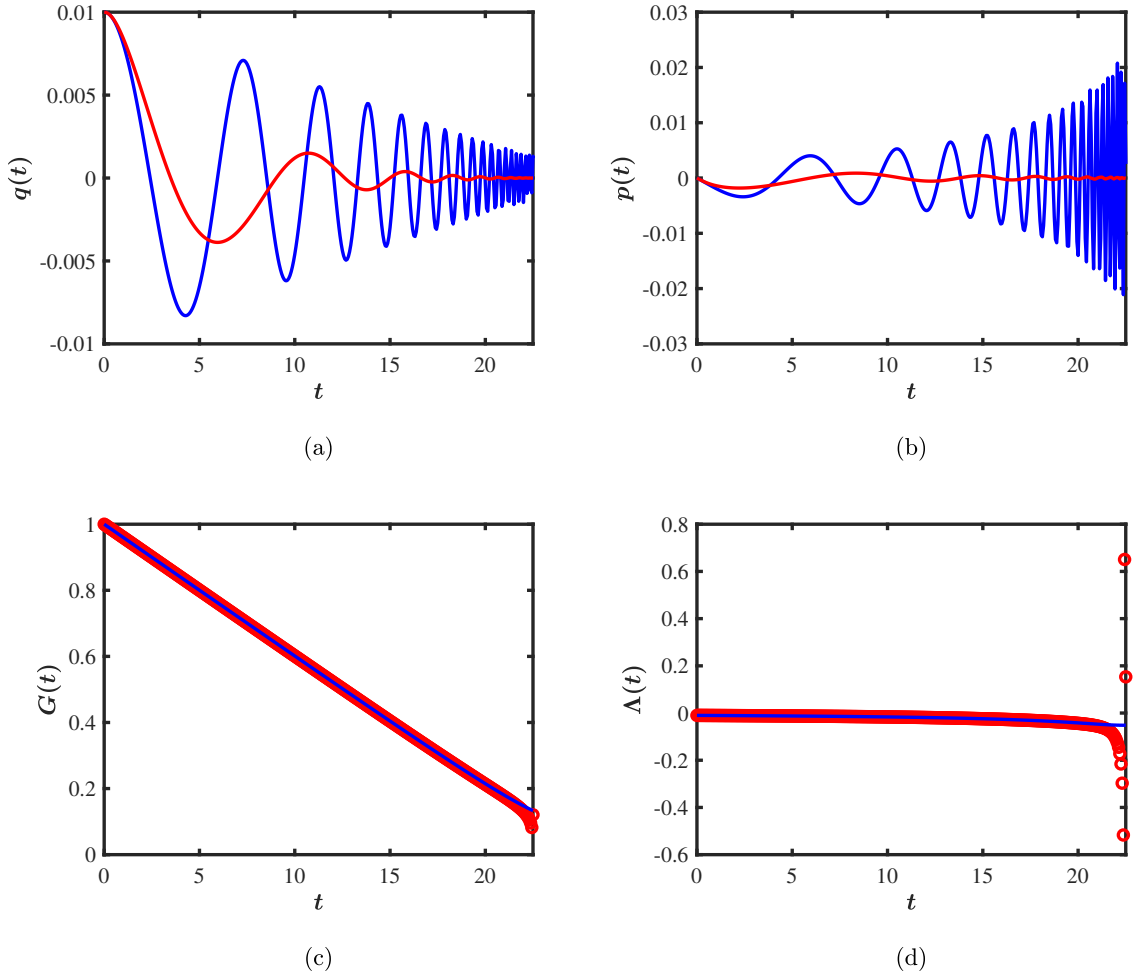

Figure 11. Dynamics when $\kappa = 2$ with $q_0 = 0.01$, $p_0 = 0$, $G_0 = 1$, and $\Lambda_0 = -0.01$. The numerical results (with $L = 80$) are in red, and the variational results are in blue. Both solutions fail at the blowup time around $t \approx 22.5$. Again, the results from numerical simulations for the variables $G(t)$ and $\Lambda(t)$ are shown with red open circles to ease visualization.

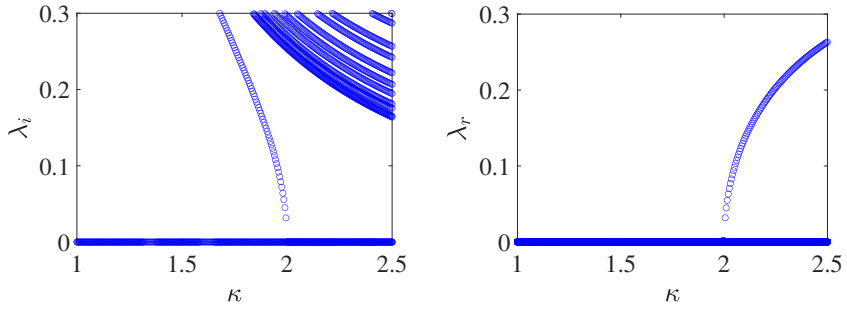

Figure 12. The imaginary λ_i (left) and real λ_r (right) parts of the eigenvalue λ as functions of κ with $g = 1$ and $\beta = 1$. At the critical value of $\kappa_c = 2$, the solution [cf. Eq. (2.3)] becomes unstable.

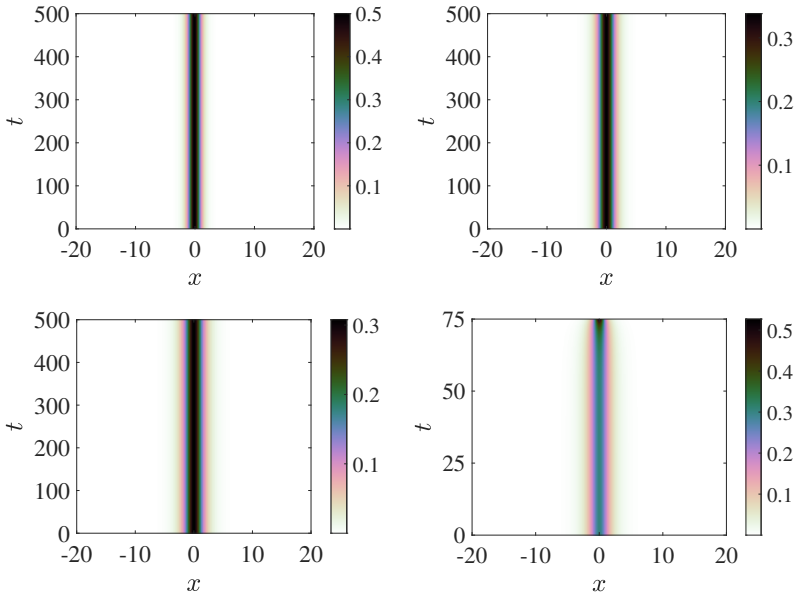

Figure 13. Spatio-temporal evolution of the density $|\psi|^2$ for different values of κ: $\kappa = 1$ (top left), $\kappa = 1.5$ (top right), $\kappa = 1.95$ (bottom left), and $\kappa = 2.1$ (bottom right).

9. Conclusions

In this work, we have considered the stability of the trapped soliton solution of a generalized Manakov system of two coupled NLSEs with the particular constraint $\psi_2(x,t) = \psi_1(-x,t)$ both numerically and analytically, and in a four collective coordinate (4CC) approximation for arbitrary nonlinearity parameter κ. We were able to show that this system is equivalent to a nonlocal NLSE (i.e., NNLSE) derivable from a nonlocal action. We found by a variety of methods, that the stability to width changes of this NNLSE had exactly the same behavior as the counterpart single component NLSE. That is, for $\kappa < 2$ there is stability, for $\kappa > 2$ there is instability (either collapse or blowup), and at $\kappa = 2$, the solution is at the critical mass and the solution blows up or collapses linear in time when perturbed. Unlike the NLSE which has Galilean invariance and a conserved momentum which can be nonzero, the NNLSE has zero value for the conserved momentum. This leads to a different response to shifting the initial conditions on the wave function to be centered slightly away from the origin.

When we shift the trapped "solitary wave" solution slightly from the origin, the ensuing oscillations of the solitary wave are reasonably well captured by the 4CC approximation which violates parity conservation. We find no evidence numerically or in the 4CC approximation of any translation instability. However, in the unstable regime, i.e., $\kappa \geq 2$, a slight translation causes the wave function to collapse. When one is in the blowup regime, having $q_0 \neq 0$ accelerates the blowup. These phenomena are quite different than what are found for the NLSE. In conclusion, we have mapped

out the stability regions for the NNLSE with arbitrary nonlinearity parameter κ, and have studied the response of the exact solutions both analytically (in the realm of a CC approximation) as well as numerically, and found the two approaches are in accordance with respect to the time evolution of the width parameter. The 4CC approximation, which violates the symmetry $\psi(-x) = \psi(x)$ when $q(t) \neq 0$ gives results for $q(t)$ and $p(t)$ which are only qualitative.

Acknowledgments

We thank M. Lakshmanan (Bharathidasan University) for useful correspondence. EGC, FC, and JFD would like to thank the Santa Fe Institute and the Center for Nonlinear Studies at Los Alamos National Laboratory for their hospitality. AK is grateful to Indian National Science Academy (INSA) for awarding him INSA Senior Scientist position at Savitribai Phule Pune University, Pune, India. The work of AS was supported by the U.S. Department of Energy.

Appendix A. Useful integrals and identities

For given κ, the c_1, c_2, and c_3 functions are explicitly given by

$$c_1(\gamma) = \int_{-\infty}^{+\infty} \mathrm{d}z \ \mathrm{sech}^{2\gamma}(z) = \frac{\sqrt{\pi}\,\Gamma[\gamma]}{\Gamma[\gamma + 1/2]} \,, \tag{A.1a}$$

$$\begin{aligned} c_2(\gamma) &= \int_{-\infty}^{+\infty} \mathrm{d}z \, z^2 \ \mathrm{sech}^{2\gamma}(z) \\ &= 2^{2\gamma-1} \, {}_4F_3[\gamma, \gamma, \gamma, 2\gamma; 1+\gamma, 1+\gamma, 1+\gamma; -1]/\gamma^3 \,, \end{aligned} \tag{A.1b}$$

$$\begin{aligned} c_3(\gamma) &= \int_{-\infty}^{+\infty} \mathrm{d}z \ \mathrm{sech}^{2\gamma}(z) \ \tanh^2(z) \\ &= c_1(\gamma) - c_1(\gamma+1) = \frac{c_1(\gamma)}{2\gamma+1} \,, \end{aligned} \tag{A.1c}$$

where ${}_4F_3$ is a hypergeometric function (see also the top panels of Fig. A1 for the dependence of c_1 and c_2 on γ). A useful result is

$$\frac{c_1(\gamma+1)}{c_1(\gamma)} = \frac{2\gamma}{2\gamma+1} \,. \tag{A.2}$$

We have defined the integral $f(z, \kappa)$ in (6.8):

$$f(z,\gamma) = \frac{2\gamma+1}{2^{1/\gamma+2}\,\gamma\,c_1(\gamma)} \int \mathrm{d}y \, [\ \mathrm{sech}^{2\gamma}(y-z) + \ \mathrm{sech}^{2\gamma}(y+z)\,]^{1/\gamma+1} \,. \tag{A.3}$$

Then

$$f(0,\gamma) = \frac{2\gamma+1}{2\gamma\,c_1(\gamma)} \int \mathrm{d}y \ \mathrm{sech}^{2\gamma+2}(y) = \frac{2\gamma+1}{2\gamma} \, \frac{c_1(\gamma+1)}{c_1(\gamma)} = 1 \,. \tag{A.4}$$

Plots of $f(z,\gamma)$ are shown in the bottom left panel of Fig. A1. The derivative of $f(z,\gamma)$ wrt z is given by

$$f'(z,\gamma) = \frac{(\gamma+1)(2\gamma+1)}{2^{1/\gamma+1}\gamma\,c_1(\gamma)} \int \mathrm{d}y \, [\ \mathrm{sech}^{2\gamma}(y-z) + \ \mathrm{sech}^{2\gamma}(y+z)\,]^{1/\gamma} \tag{A.5}$$

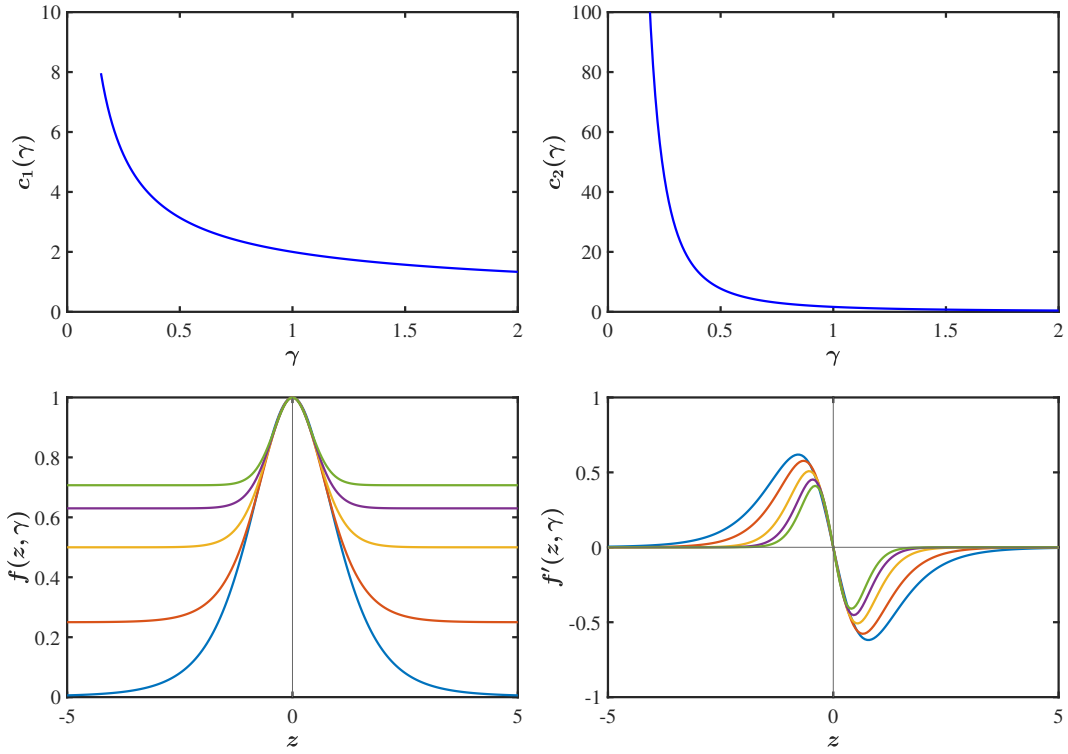

Figure A1. The top panels present $c_1(\gamma)$ (left panel) and $c_2(\gamma)$ (right panel) as a function of γ (for their definition, see Eqs. (A.1a) and (A.1b), respectively). The bottom panels demonstrate the dependence of $f(z,\gamma)$ (left panel), and $f'(z,\gamma)$ (right panel) on z, and for various values of $\gamma = 0.1, 0.5, 1, 1.5$, and 2 depicted by solid blue, orange, yellow, purple, and green lines, respectively (see Eqs. (A.3) and (A.5), respectively).

$$\times \left[\operatorname{sech}^{2\gamma}(y-z)\tanh(y-z) - \operatorname{sech}^{2\gamma}(y+z)\tanh(y+z) \right],$$

where $f'(0,\gamma) = 0$. Plots of $f'(z,\gamma)$ are shown in the bottom right panel of Fig. A1. A short calculation using Mathematica gives

$$f''(0,\gamma) = -4\,\frac{\gamma+1}{2\gamma+3}\,. \tag{A.6}$$

Expanding $f(z,\gamma)$ about the origin gives

$$f(z,\gamma) = f(0,\gamma) + f'(0,\gamma)\,z + \frac{1}{2}\,f''(0,\gamma)\,z^2 + \cdots = 1 - 2\,\frac{\gamma+1}{2\gamma+3}\,z^2 + \cdots\,, \tag{A.7a}$$

$$f'(z,\gamma) = -4\,\frac{\gamma+1}{2\gamma+3}\,z + \cdots\,. \tag{A.7b}$$

Appendix B. Moments and collective coordinates

The variational wave function of Eq. (6.1) is of the form

$$\psi(x,t) = \Big[\, \frac{M}{G(t)\, c_1(\gamma)} \,\Big]^{1/2} \, \mathrm{sech}^{\gamma}\Big[\, \frac{x - q(t)}{G(t)} \,\Big]\, \mathrm{e}^{\mathrm{i}\phi(x,t)} \,, \tag{B.1a}$$

$$\phi(x,t) = p(t)\,(x - q(t)) + \Lambda(t)\,(x - q(t))^2 \,. \tag{B.1b}$$

Let us define the n^{th} moment of the density distribution by

$$\begin{aligned} M_n(t) &= \int_{-\infty}^{+\infty} \mathrm{d}x\, x^n \,|\, \psi(x,t) \,|^2 \\ &= \frac{M}{G(t)\, c_1(\gamma)} \int_{-\infty}^{+\infty} \mathrm{d}x\, x^n \, \mathrm{sech}^{2\gamma}[\,(\,x - q(t)\,)/G(t)\,] \\ &= \frac{M}{c_1(\gamma)} \int_{-\infty}^{+\infty} \mathrm{d}y\, [\, G(t)\, y + q(t)\,]^n \, \mathrm{sech}^{2\gamma}(y) \,. \end{aligned} \tag{B.2}$$

Explicitly, we find:

$$M_0(t) = M \,, \tag{B.3a}$$

$$M_1(t) = M\, q(t) \,, \tag{B.3b}$$

$$M_2(t) = M \left[\, q^2(t) + G^2(t)\, \frac{c_2(\gamma)}{c_1(\gamma)} \,\right] , \tag{B.3c}$$

from which we can find $q(t)$ and $G(t)$. The zeroth moment, i.e., the mass of the soliton must be conserved. In a similar way, let us define the n^{th} moment of the momentum distribution by

$$\begin{aligned} P_n(t) &= \frac{1}{2\mathrm{i}} \int_{-\infty}^{+\infty} \mathrm{d}x\, x^n \left[\, \psi^*(x,t)\, \frac{\partial \psi(x,t)}{\partial x} - \frac{\partial \psi^*(x,t)}{\partial x}\, \psi(x,t) \,\right] \\ &= \int_{-\infty}^{+\infty} \mathrm{d}x\, x^n \, \mathrm{Im}\Big\{\, \psi^*(x,t)\, \frac{\partial \psi(x,t)}{\partial x} \,\Big\} = \int_{-\infty}^{+\infty} \mathrm{d}x\, x^n \, \frac{\partial \phi(x,t)}{\partial x} \,|\, \psi(x,t) \,|^2 \\ &= \int_{-\infty}^{+\infty} \mathrm{d}x\, x^n \,\{\, p(t) + 2\,\Lambda(t)\,[x - q(t)]\,\} \,|\, \psi(x,t) \,|^2 \\ &= \frac{M}{G(t)\, c_1(\gamma)} \int_{-\infty}^{+\infty} \mathrm{d}x\, x^n \,\{\, p(t) + 2\,\Lambda(t)\,[x - q(t)]\,\} \, \mathrm{sech}^{2\gamma}[(x - q(t))/G(t)] \\ &= \frac{M}{c_1(\gamma)} \int_{-\infty}^{+\infty} \mathrm{d}y\, [\, q(t) + G(t)\, y\,]^n \,[\, p(t) + 2\,\Lambda(t)\, G(t)\, y\,] \, \mathrm{sech}^{2\gamma}(y) \,. \end{aligned} \tag{B.4}$$

Explicitly, we find:

$$P_0(t) = M\, p(t) \,, \tag{B.5a}$$

$$P_1(t) = M \left[\, p(t)\, q(t) + 2\,\Lambda(t)\, G^2(t)\, \frac{c_2(\gamma)}{c_1(\gamma)} \,\right] . \tag{B.5b}$$

This way, $p(t)$ can be obtained from (B.5a), and $\Lambda(t)$ from:

$$\Lambda(t) = \frac{1}{2\, G^2(t)} \left[\, \frac{P_1(t)}{M} - p(t)\, q(t) \,\right] \frac{c_1(\gamma)}{c_2(\gamma)} \,. \tag{B.6}$$

References

[1] P.G. Kevrekidis and D.J. Frantzeskakis, Solitons in coupled nonlinear Schrödinger models: A survey of recent developments, *Rev. Phys.* **1** (2016), 140. https://doi.org/10.1016/j.revip.2016.07.002.

[2] M.J. Ablowitz and B. Prinari, Nonlinear Schrödinger systems: continuous and discrete., *Scholarpedia* **3**(8) (2008), 5561.

[3] H.A. Rose and M.I. Weinstein, On the bound states of the nonlinear schrödinger equation with a linear potential, *Physica D: Nonlinear Phenomena* **30**(1) (1988), 207–218. doi:https://doi.org/10.1016/0167-2789(88)90107-8. http://www.sciencedirect.com/science/article/pii/0167278988901078.

[4] F. Cooper, C. Lucheroni and H. Shepard, Variational method for studying self-focusing in a class of nonlinear Schrödinger equations, *Physics Letters A* **170**(3) (1992), 184–188. doi:https://doi.org/10.1016/0375-9601(92)91063-W. http://www.sciencedirect.com/science/article/pii/037596019291063W.

[5] F. Cooper, H. Shepard, C. Lucheroni and P. Sodano, Post-Gaussian variational method for the nonlinear Schrödinger equation: Soliton behavior and blowup, *Physica D: Nonlinear Phenomena* **68**(3) (1993), 344–350. doi:https://doi.org/10.1016/0167-2789(93)90129-O. http://www.sciencedirect.com/science/article/pii/016727899390129O.

[6] F. Cooper, J.F. Dawson, F.G. Mertens, E. Arévalo, N.R. Quintero, B. Mihaila, A. Khare and A. Saxena, Response of exact solutions of the nonlinear Schrödinger equation to small perturbations in a class of complex external potentials having supersymmetry and parity-time symmetry, *Journal of Physics A: Mathematical and Theoretical* **50**(48) (2017), 485205.

[7] N.R. Quintero, F.G. Mertens and A.R. Bishop, Generalized traveling-wave method, variational approach, and modified conserved quantities for the perturbed nonlinear Schrödinger equation, *Phys. Rev. E* **82** (2010), 016606. doi:10.1103/PhysRevE.82.016606.

[8] F. Cooper, A. Khare, A. Comech, B. Mihaila, J.F. Dawson and A. Saxena, Stability of exact solutions of the nonlinear Schrödinger equation in an external potential having supersymmetry and parity-time symmetry, *J. Phys. A: Math. Theor.* **50** (2017), 015301.

[9] E.G. Charalampidis, J.F. Dawson, F. Cooper, A. Khare and A. Saxena, Stability and response of trapped solitary wave solutions of coupled nonlinear Schrödinger equations in an external $\mathcal{PT}$- and supersymmetric potential, *Journal of Physics A: Mathematical and Theoretical* **53**(45) (2020), 455702. doi:10.1088/1751-8121/abb278.

[10] E.G. Charalampidis, F. Cooper, J.F. Dawson, A. Khare and A. Saxena, Behavior of solitary waves of coupled nonlinear Schrödinger equations subjected to complex external periodic potentials with odd-PT symmetry, *Journal of Physics A: Mathematical and Theoretical* **54**(14) (2021), 145701. doi:10.1088/1751-8121/abdca8.

[11] S.V. Manakov, On the theory of two-dimensional stationary self-focusing of electromagnetic waves, *Zh. Eksp. Teor. Fix.* **65** (1973), 505, [Sov. Phys. JETP 38, 248 (1974)].

[12] C.R. Menyuk, Nonlinear pulse propagation in birefringent optical fibeers, *IEEE J. Quant. Electr.* **23** (1987), 174.

[13] V.V. Konotop and D.A. Zezyulin, Spectral singularities of odd-$\mathcal{PT}$-symmetric potentials, *Phys. Rev. A* **99** (2019), 013823. doi:10.1103/PhysRevA.99.013823.

[14] J. Ablowitz and Z.H. Musslimani, Integrable nonlocal nonlinear Schrödinger equation, *Phys. Rev. Lett.* **110** (2013), 064105.

[15] J. Yang, Physically significant nonlocal nonlinear Schrödinger equation and its soliton solutions, *Phys. Rev. E* **98** (2018), 042202. doi:10.1103/PhysRevE.98.042202.

[16] M.J. Ablowitz and Z.H. Musslimani, Inverse scattering transform for the integrable nonlocal nonlinear Schrödinger equation, *Nonlinearity* **29**(3) (2016), 915–946. doi:10.1088/0951-7715/29/3/915.

[17] V.S. Gerdjikov and A. Saxena, Complete integrability of nonlocal nonlinear Schrödinger equation,

Journal of Mathematical Physics **58**(1) (2017), 013502.

[18] S. Stalin, R. Ramakrishnan and M. Lakshmanan, Nondegenerate soliton solutions in certain coupled nonlinear Schrödinger systems, *Physics Letters A* **384**(9) (2020), 126201. doi:https://doi.org/10.1016/j.physleta.2019.126201.

[19] M. Gurses and A. Pekcan, Nonlocal nonlinear Schrödinger equations and their soliton solutions, *Journal of Mathematical Physics* **59**(5) (2018), 051501.

[20] W. Liu and X. Li, General soliton solutions to a (2+1)-dimensional nonlocal nonlinear Schrödinger equation with zero and nonzero boundary conditions, *Nonlinear Dynamics* **93**(2) (2018), 721–731.

[21] B. Yang and Y. Chen, Dynamics of high-order solitons in the nonlocal nonlinear Schrödinger equation, *Nonlinear Dynamics* **94**(1) (2018), 489–502.

[22] K. Manikandan, S. Stalin and M. Senthilvelan, Dynamical behaviour of solitons in a invariant nonlocal nonlinear Schrödinger equation with distributed coefficients, *European Physical Journal B* **91**(11) (2018), 291.

[23] B.-F. Feng, X.-D. Luo, M.J. Ablowitz and Z.H. Musslimani, General soliton solution to a nonlocal nonlinear Schrödinger equation with zero and nonzero boundary conditions, *Nonlinearity* **31**(12) (2018), 5385–5409.

[24] N.V. Priya, M. Senthilvelan, G. Rangarajan and M. Lakshmanan, On symmetry preserving and symmetry broken bright, dark and antidark soliton solutions of nonlocal nonlinear Schrödinger equation, *Phys. Lett. A* **383**(1) (2019), 15–26.

[25] J. Yang, General N-solitons and their dynamics in several nonlocal nonlinear Schrödinger equations, *Phys. Lett. A* **383**(4) (2019), 328–337.

[26] S. Stalin, M. Senthilvelan and M. Lakshmanan, Energy-sharing collisions and the dynamics of degenerate solitons in the nonlocal Manakov system, *Nonlinear Dynamics* **95**(3) (2019), 1767–1780.

[27] Y. Rybalko and D. Shepelsky, Long-time asymptotics for the integrable nonlocal nonlinear Schrödinger equation, *J. Math. Phys.* **60**(3) (2019), 031504.

[28] T. Xu, S. Lan, M. Li, L.-L. Li and G.-W. Zhang, Mixed soliton solutions of the defocusing nonlocal nonlinear Schrödinger equation, *Physica D: Nonlinear Phenomena* **390** (2019), 47–61.

[29] T. Xu, Y. Chen, M. Li and D.-X. Meng, General stationary solutions of the nonlocal nonlinear Schrödinger equation and their relevance to the PT-symmetric system, *Chaos* **29**(12) (2019), 123124.

[30] D. Wang, Y. Huang, X. Yong and J. Zhang, Rational soliton solutions of the nonlocal nonlinear Schrödinger equation by the KP reduction method, *Int. J. Mod. Phys. B* **33**(30) (2019), 1950362.

[31] G.H. Derrick, Comments on Nonlinear Wave Equations as Models for Elementary Particles, *Journal of Mathematical Physics* **5**(9) (1964), 1252–1254. doi:10.1063/1.1704233.

[32] F. Cooper, J.F. Dawson, F.G. Mertens, E. Arévalo, N.R. Quintero, B. Mihaila, A. Khare and A. Saxena, Response of exact solutions of the nonlinear Schrödinger equation to small perturbations in a class of complex external potentials having supersymmetry and parity-time symmetry, *Journal of Physics A: Mathematical and Theoretical* **50**(48) (2017), 485205. doi:10.1088/1751-8121/aa8d25.

[33] J.F. Dawson, F. Cooper, A. Khare, B. Mihaila, E. Arévalo, R. Lan, A. Comech and A. Saxena, Stability of new exact solutions of the nonlinear Schrödinger equation in a Pöschl–Teller external potential, *Journal of Physics A: Mathematical and Theoretical* **50**(50) (2017), 505202.

[34] https://www.mathworks.com/help/matlab/ref/ode113.html.

[35] A.-K. Kassam and L.N. Trefethen, Fourth-order time-stepping for stiff PDEs, *SIAM J. Sci. Comput.* **26**(4) (2005), 1214–1233. doi:10.1137/S1064827502410633.

[36] C.T. Kelley, *Solving Nonlinear Equations with Newton's Method*, Fundamentals of Algorithms, Society for Industrial and Applied Mathematics (SIAM), Philadelphia, 2003.

[37] C. Sulem and P.L. Sulem, *The Nonlinear Schrödinger Equation: Self-Focusing and Wave Collapse*, Applied Sciences, Springer-Verlag, New York, 1999.

[38] C.I. Siettos, I.G. Kevrekidis and P.G. Kevrekidis, Focusing revisited: a renormalization/bifurcation approach, *Nonlinearity* **16**(2) (2003), 497–506. doi:10.1088/0951-7715/16/2/308.